Path Following and Output Synchronization of Homogeneous Linear Time-Invariant Systems

by

Maxwell Steinfeld

A thesis
presented to the University of Waterloo
in fulfillment of the
thesis requirement for the degree of
Master of Applied Science
in
Electrical & Computer Engineering

Waterloo, Ontario, Canada, 2018

I hereby declare that I am the sole author of this thesis. This is a true copy of the thesis, including any required final revisions, as accepted by my examiners.

I understand that my thesis may be made electronically available to the public.

Abstract

This thesis examines two aspects of the path following control design problem for L.T.I. systems assigned closed curves in their output space. In the first part of the thesis we define a path following normal form for L.T.I. systems and study structural properties related to this normal form. We isolate how unstable zero dynamics alter the feasibility of using the path following normal form for control design. In the second half of the thesis we consider a synchronized path following problem for a homogenous multi-agent system and cast the problem as an instance of an output synchronization problem to leverage recent results from the literature. It is desired that each individual agent follow a specified path. The agents communicate with one another over an idealized communication network to synchronize their positions along the path. The main result is the construction of a dynamic feedback coupling that drives all the agents in the network to their respective reference paths while simultaneously synchronizing their positions along the path. Laboratory results are presented to illustrate the effectiveness of the proposed approach.

Acknowledgements

I would like to first thank my advisor Professor Christopher Nielsen for his guidance, advice and feedback. I would also like to thank Professor Baris Fidan for granting access to his lab with a motion capture system and Professor Steven Waslander for providing two autonomous mobile robots, without which no experimental data could be obtained. I would like to thank my friends for their help through stressful times. Lastly, I thank my family whom have always been there to pick me up and push me to achieve my potential.

Table of Contents

List of Tables

List of Figures

List of Abbreviations

I.M.P. Internal Model Principle 6

I.R. Infrared 82

L.T.I. Linear Time-Invariant iii, 1, 3, 4, 6–8, 14–16, 37, 56, 72

M.A.S. Multi-Agent System 7, 73, 91, 95–97

M.I.M.O. Multi-Input Multi-Output 15

N.M.P. Non-Minimum Phase 2, 4, 6, 95, 96

R.O.S. Robot Operating System 74

S.I.S.O. Single-Input Single-Output 15

Chapter 1

Introduction

The path following control design problem entails designing feedback controllers that drive output trajectories of the closed-loop system towards an assigned path while moving along the path in a desirable and application specific manner. An important property of path following controllers, sharply distinguishing them from trajectory tracking controllers, is that the path can be made invariant for the closed-loop system. That is, unlike a tracking controller, a path following controller stabilizes a family of trajectories, all of whose associated output signals can be made to lie on the assigned path for all time. This familty of trajectories is partially determined by the zero dynamics of the control system.

In this thesis, two aspects of the path following control design problem are investigated. In the first part of the thesis, we define a path following normal form for L.T.I. systems and study structural properties related to this normal form. We isolate how unstable zero dynamics alter the feasibility of using the path following normal form for controller design. We present a solution for the path following problem that leverages the fact that closed curves are diffeomorphic to unit circles. With respect to unstable zero dynamics, while

there are known results for reducing performance limitations for N.M.P. systems [1],[26], we ultimately find that they are not amenable to be leveraged with the path following normal form.

The second probelm considered is a synchronized path following problem [9, 25]. Each agent is assigned a (possibly distinct) closed curve in its output space. The agent must use its own state and path information to drive its output to the path while ensuring output invariance of the path. At the same time, the agents must, by exchanging information between themselves, synchronize their position along the path with other agents. Unlike previous works [9, 25], synchronization is not modelled as a constraint on the allowable motions along the path and instead an output synchronization problem [37], [41] is solved for the dynamics governing the tangential motion along the paths.

1.1 Motivating Applications

With the Google self-driving car having crossed the million mile mark [35] and Tesla safety features, including some limited auto-pilot features, it is clear that self-driving cars will soon become commercially available in the near future. Fundamental to the problem of self-driving cars is their ability to communicate and coordinate with one another for safety and speed. In this application having the vehicle stay in its lane on a road could represent the primary objective of driving the system output to a pre-assigned path. Invariance of the path is important because if the road were too curvy, then there is a potential to leave the lane traveling at high speed. Once in a lane, it is desirable to maintain a minimum speed and inter-vehicle distance. From a path following prospective, this is the secondary objective. Path following controllers can decouple the design of controllers to achieve these objectives.

A second motivating application of path following controllers is the control of a fleet of aerial robots designed for enhanced image resolution; popular in fields such as surveillance, reconnaissance and astrology. Typically, multiple photographs will be taken of an interested area but at different attitudes and positions. An image can then be produced by aggregating all of the pictures taken concurrently. In this arrangement, different reference trajectories could be given in order to have the variation needed with regards to the field of views. The closer the robots are to one another, the more overlap each frame will have, producing better estimates for the final image. If the robots are close to one another invariance of their paths will avoid collisions. The secondary objective could then be used to maintain an equal distance from the target area from the cameras point of view.

1.2 Literature Review

1.2.1 Performance Limitations

A common task for controllers is reference tracking wherein the output of a system, $y(t)$, is made to follow a specified trajectory, $r(t)$. A measure of how well the controller performs can be taken to be the $\mathcal{L}_2-$norm of the tracking error

$$\begin{aligned} J &= \int_0^\infty \|y(t) - r(t)\|^2 \mathrm{d}t \\ &= \int_0^\infty \|e(t)\|^2 \mathrm{d}t. \end{aligned}$$

The tracking error, $e(t)$, is the difference between the system output and a reference signal. The above cost function does not take into account the control effort used. It can be shown that for stabilizable L.T.I. minimum phase systems, it is possible to make the cost function

arbitrarily small [22]. If a system is N.M.P. it is well known that there will be difficulties in making the error approach zero and with unstable zero dynamics there is a fundamental limitation on the attainable performance [36]. The minimal value of

$$J_\rho = \int_0^\infty \left[e^\top(t)Me(t) + \rho u^\top(t)Nu(t)\right] \mathrm{d}t \tag{1.1}$$

where M and N are symmetric positive-definite matrices, is lower bounded by a strictly positive number as $\rho \to 0$ [22]. To overcome this limitation, a reformulation of the tracking problem is considered, known as path following. In path following, one introduces a timing law, $\theta(t)$, which creates an extra degree of freedom. The timing law is composed with the reference, $r(\theta(t))$, which allows the time derivative of the reference signal to be manipulated in order to achieve better performance. Performance is improved by including the timing law in the tracking error to obtain the path following error

$$e_{\mathrm{PF}}(t) = y(t) - r(\theta(t)).$$

The path following error is the difference between the system output and the modified reference signal.

A. Aguir [1] presented a path following formulation of the tracking task by dividing the objective into two tasks: geometric path following and speed assignment along the path. The paths considered are linear combinations of sinusoids for a class of L.T.I. N.M.P. systems. In his formulation, the controller objectives are:

(i) Boundedness: the plant states stay uniformly bounded for every initial condition as $t \to \infty$

(ii) Error convergence: $e_{\mathrm{PF}}(t) \to 0$ as $t \to \infty$

(iii) Forward motion: $\dot{\theta}(t) > v_d$ for all $t > 0$ where v_d is a positive constant

(iv) If given a desired speed $v_d > 0$, then $\dot{\theta}(t) \to v_d$ as $t \to \infty$

A. Aguir is interested in determining whether or not the extra degree of freedom introduced by the timing law can be used to attain an arbitrarily small $\mathcal{L}_2-$norm of the path following error. Using the results of Qiu and Davison [36], Aguir shows that although the ideal performance cannot be reached, the cost function (1.1) can still be made less than an arbitrarily small positive constant δ. The best attainable performance shown is shown to be

$$J = \sum_{i=1}^{p} \sum_{j=1}^{q} \left(\frac{1}{z_i - j v_d w_j} + \frac{1}{z_i + j v_d w_j} \right)$$

where z_i are the zeros of the system in the right-half plane and $w_j > 0$ are real numbers dependent on the path. When given a desired speed instead of requiring forward motion only, a piecewise constant timing law is introduced:

$$\aleph : [0, \infty) \to \{0, 1, 2, \ldots, N\}$$

$$\aleph(t) := \begin{cases} 0, & t_0 \leq t < t_1 \\ 1 & t_1 \leq t < t_2 \\ \vdots & \\ N, & t \geq t_N. \end{cases}$$

Each case of the timing law has its own specified velocity with each value being less than the previous until the desired speed is reached. A. Aguir includes constraints on the time between steps, step size and initial velocity in order to provide arbitrarily good performance. Later on, his work is extended to include nonlinear systems [2]. The same

concepts are used and applied to the nonlinear version under some mild assumptions and the results are the same. By reformulating the tracking task as a path following problem, the system is no longer subject to the limitations of tracking and an arbitrarily small $\mathcal{L}_2-$norm of the path following error can be achieved.

D. Miller and R. Middleton also look at L.T.I. N.M.P. systems and are interested in determining the class of trajectories for which the path following cost can be made arbitrarily small [26]. In cases where it is non-zero, it is shown how the optimal cost, in the sense of the $\mathcal{L}_2-$norm of the path following error, can be computed as the solution to a finite dimensional convex optimization problem. A method for calculating upper and lower bounds on the attainable performance is also provided.

1.2.2 Output Synchronization

In recent years, coordination and path following problems have received increasing attention amongst systems and control researchers. This is largely due to the abundance of applications in physics and engineering. Coordination problems are interested in having all the agents of a network collectively agree on parameters of interest. Coordination can be decomposed further into consensus or synchronization problems.

Synchronization problems focus primarily on the individual agent's dynamics rather than the communication constraints imposed on agents. The communication graph is assumed to be time-invariant and the agent's dynamics may be influenced via the exchange of information. The key goal is for all individual agents to converge asymptotically to some common trajectory [37].

One method for achieving synchronization is to use the I.M.P.. The I.M.P. tells us necessary and sufficient conditions for a tracking problem to be solvable. Essentially, it

says that the controller must incorporate the dynamic structure of the disturbance and reference signals into its design in order for perfect tracking to be made possible. It was first introduced by B. Francis and W. Wonham in 1976 [12]. They consider a class of L.T.I. systems with deterministic disturbance and reference signals. The unstable poles of the disturbance and reference signals are canceled to provide closed-loop stability.

P. Wieland uses these results in order to solve a synchronization path following problem for an L.T.I. M.A.S. [41]. The main contribution made is the extension of necessary and sufficient conditions for uniformly exponential sychronizability to a heterogeneous M.A.S. equipped with a communication graph that may be time-varying, intermittent and directional. It is shown that a common exosystem is required amongst all systems in the network, designated the virtual exosystem, in order for synchronization to be achieved. This distinguishes his work from A. Doosthoseini [10] where synchronization is achieved by constraining the allowable motions of the system once it has reached the required path.

1.3 Notation

The symbol $\coloneqq$ means equal by definition. Transpose is denoted by $\top$. The complex plane $\mathbb{C}$ is partitioned as $\mathbb{C} = \mathbb{C}^- \cup \mathbb{C}^+$, where $\mathbb{C}^- \coloneqq \{s \in \mathbb{C} : \mathrm{Re}(s) < 0\}$ and $\mathbb{C}^+ \coloneqq \{s \in \mathbb{C} : \mathrm{Re}(s) \geq 0\}$. The $n \times n$ identity matrix is denoted by I_n. For a vector $x \in \mathbb{R}^n$ the symbol $\|x\|$ denotes the Euclidean norm, i.e., $\|x\| = \sqrt{x^\top x}$. Let $B_\delta(p) = \{x \in \mathbb{R}^n : \|x - p\| < \delta\}$ denote the open ball of radius $\delta > 0$ centred at a point $p \in \mathbb{R}^n$. Given $N \in \mathbb{N}$, let $\mathbb{N}_N \coloneqq \{1, 2, 3, \ldots, N\}$. If $L > 0$ and real, then the notation $\mathbb{R} \bmod L$ represents the real numbers modulo L. Let $\arg : \mathbb{C} \to (-\pi, \pi]$ map a complex number to its principal argument. The symbol $\otimes$ denotes the Kronecker product.

Given a matrix S, the spectrum of S is denoted $\sigma(S)$. Given a function $\sigma : A \to B$,

we will either write $\sigma(A)$ or $\mathrm{Im}(\sigma)$ to denote its image. If $\phi : \mathbb{R}^n \to \mathbb{R}^m$ is a smooth map, then we will use either $\mathrm{d}\phi_{\bar{x}}$ or $\frac{\partial \phi}{\partial x}\big|_{x=\bar{x}}$ to denote its Jacobian evaluated at $\bar{x} \in \mathbb{R}^n$. If f, $g : \mathbb{R}^n \to \mathbb{R}^n$ are smooth vector fields, we use the following standard notation for iterated Lie derivatives $L_f^0\phi(x) := \phi(x)$, $L_f^k\phi(x) := L_f(L_f^{k-1}\phi)(x) = \frac{\partial L_f^{k-1}\phi}{\partial x} f(x)$, $L_g L_f \phi(x) := L_g(L_f\phi)(x) = \frac{\partial L_f \phi}{\partial x} g(x)$.

1.4 Contributions

The main contributions of this thesis are:

1. A detailed study of the path following normal form and its relationship to zero dynamics.

2. The use of recent results in the synchronization literature to solve a synchronized path following problem for L.T.I. systems.

3. Laboratory results using physical systems in order to illustrate the effectiveness of the proposed control algorithm.

4. Formal proof that the relative degree of a system at a point does not change when we apply a diffeomorphism to the output space.

Chapter 2

Background

The main purpose of this chapter is to collect some definitions and results used extensively throughout the thesis in one location. The contents in the rest of the thesis draw heavily from the ideas presented here.

2.1 Mathematical Preliminaries

First we recall a few basic definitions from calculus on real finite-dimensional vector spaces.

Definition 2.1.1. A subset A of $\mathbb{R}^n$ is open if, for every point p in A, there exists a $\delta > 0$ such that $B_\delta(p) \subseteq A$. An open set containing a point $p \in \mathbb{R}^n$ is called a **neighbourhood** of p. ⧫

It immediately follows from this definition that $B_\delta(p)$ is itself an open set. The systems and mappings considered in this thesis are all smooth.

Definition 2.1.2. Consider a function $f : A \to \mathbb{R}$ where $A \subseteq \mathbb{R}^n$ is an open set. The function f is said to be **smooth** (or C^∞ or infinitely differentiable) if it possesses continuous partial derivatives of all orders. A function $f : A \to B$ where $A \subseteq \mathbb{R}^n$ and $B \subseteq \mathbb{R}^m$ are open sets is said to be smooth if each of its component functions is smooth. ⧫

In this thesis we apply nonlinear coordinate changes to time-invariant control systems. These nonlinear coordinate changes are also known as diffeomorphisms.

Definition 2.1.3. Consider a function $f : A \to B$ where $A \subseteq \mathbb{R}^n$ and $B \subseteq \mathbb{R}^m$ are open sets. The function f is a **diffeomorphism** if it is bijective, smooth and its inverse $f^{-1} : B \to A$ is also smooth. ⧫

Checking whether or not a smooth function is a diffeomorphism in a neighbourhood of a given point can be done using the classical inverse function theorem.

Theorem 2.1.4 ([32, Theorem 2.11])**.** *Let $A \subseteq \mathbb{R}^n$ be an open set and let $f : A \to \mathbb{R}^n$ be a smooth map. If the Jacobian matrix $\mathrm{d}f_p$ is non-singular at some point $p \in A$, then there exists an open set $U \subseteq A$ containing p such that $f : U \to f(U) \subseteq \mathbb{R}^n$ is a diffeomorphism.*

Definition 2.1.5. Let R be a ring and let M be a left R-module. Choose a nonempty subset S of M. The **annihilator** of S is the set of all elements $r \in R$ such that

$$rs = 0, \qquad (\forall s \in S).$$

Now we give a basic definition from control theory on stability.

Definition 2.1.6. A matrix $A \in \mathbb{R}^{n\times n}$ is **stable**, or **Hurwitz**, if all its eigenvalues are in the open left-half plane, $\sigma(A) \subset \mathbb{C}^-$. If a matrix is not stable, then it is **unstable**. ⧫

2.2 Signed Circular Distance

This thesis is concerned with path following on closed curves. At various times we will need to measure distance along these curves. Computing distances along closed curves is closely related to computing distances along points on a circle.

Let $\mathcal{C}$ denote a closed, regular, non-self-intersecting curve given by a smooth (C^∞) parameterization $\sigma : \mathbb{R} \to \mathbb{R}^m$ such that $\mathcal{C} = \mathrm{Im}(\sigma)$ and, for all $\lambda \in \mathbb{R}$, $\|\sigma'(\lambda)\| \neq 0$. Since σ is regular, without loss of generality we can assume that it has a unit speed parameterization and $\|\sigma'(\lambda)\| \equiv 1$.

Let $L > 0$ denote the finite-arc length of $\mathcal{C}$. We now explicitly show how any curve $\mathcal{C}$ with the aforementioned properties is diffeomorphic to the unit circle.

We start by showing that $\mathcal{C}$ is diffeomorphic to $\mathbb{T} \coloneqq \mathbb{R} \bmod L$. The diffeomorphism between the two sets is produced as follows. Since σ is assumed to be unit-speed, it is therefore L-periodic and any two points λ and $\lambda + L$ in the domain of σ can be identified. That is we say that $\lambda_1, \lambda_2 \in \mathbb{R}$ are equivalent if $\lambda_1 - \lambda_2 = kL$ for some integer k. It is easily verified that this defines an equivalence relation and the resulting quotient set is $\mathbb{T}$. Let $[\lambda]_L \in \mathbb{T}$ denote the equivalence class containing λ. Define a map $\tilde{\sigma} : \mathbb{T} \to \mathbb{R}^m$ through the identity

$$\tilde{\sigma}([\lambda]_L) = \sigma(\lambda).$$

Now $\tilde{\sigma}$ maps $\mathbb{T}$ diffeomorphically onto $\mathcal{C}$ and has the same properties as σ: $\mathrm{Im}\,(\tilde{\sigma}) = \mathcal{C}$, $\|\tilde{\sigma}'(\cdot)\| \neq 0$.

Next we show that the set $\mathbb{T} = \mathbb{R} \bmod L$ posseses a natural differentiable structure

which makes it diffeomorphic to the unit circle

$$\mathbb{S} \coloneqq \left\{(x, y) \in \mathbb{R}^2 : x^2 + y^2 = 1\right\}.$$

A diffeomorphism between these sets is given by

$$\begin{aligned} F : \mathbb{T} &\to \mathbb{S} \\ [\lambda]_L &\mapsto (\cos(2\pi\lambda/L), \sin(2\pi\lambda/L)) \end{aligned}$$

with inverse

$$\begin{aligned} F^{-1} : \mathbb{S} &\to \mathbb{T} \\ (x, y) &\mapsto \frac{L}{2\pi}\text{atan2}(x, y) \end{aligned}$$

where atan2 is the "smart" or four quadrant arctangent function with codomain $(-\pi, \pi]$.

To compute the signed distance between two points on $\mathbb{S}$, we use the natural isomorphism between $\mathbb{R}^2$ and the complex plane $\mathbb{C}$. If $p = (x, y) \in \mathbb{S}$ then, with a slight abuse of notation, we write $p = x + jy$. Next, expressing p in polar form using Euler's Formula we can write

$$p = \mathrm{e}^{j\varphi} = \cos(\varphi) + j\sin(\varphi) \tag{2.1}$$

where $\varphi = \arg(p)$ and arg is the principle argument.

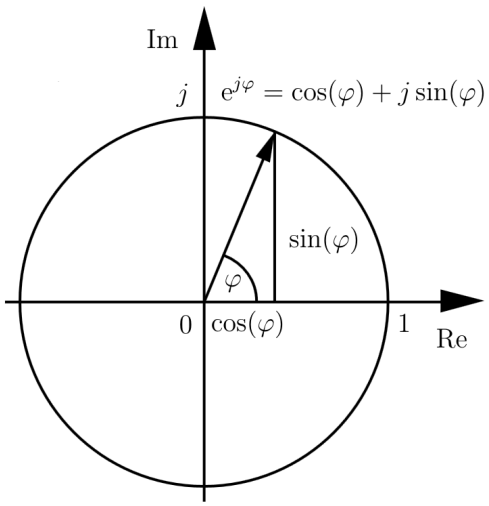

Figure 2.1: Complex Exponential Visualized

Given two points p_1 and p_2 on the $\mathbb{S}$, we define the signed distance between them as

$$\begin{aligned} \text{dist}_{\mathbb{S}} : \mathbb{S} \times \mathbb{S} &\to (-\pi, \pi] \\ (p_1, p_2) &\mapsto \arg\left(\exp\left(j(\arg\left(p_1\right) - \arg\left(p_2\right))\right)\right). \end{aligned} \tag{2.2}$$

It is easy to check that $\text{dist}_{\mathbb{S}}\left(p_1, p_2\right) = \arg\left(p_1/p_2\right)$ and $\text{dist}_{\mathbb{S}}(p_1, p_2) = -\text{dist}_{\mathbb{S}}(p_2, p_1)$.

2.3 Class of Control Systems

The first step in creating any controller is to model the dynamics of the system to be controlled. This can be done using physics and Newtons' laws of motion or empirically with experimental data. Once a mathematical model is derived it can be analyzed and used to simulate different controller designs. The controller can be tweaked within the simulation to meet specifications before implementing it on the actual system. This is

advantageous because it gives an expectation of what is to happen and many designs can be tested without the need to worry about damaging the apparatus.

A large class of control systems can be modelled as nonlinear, time-invariant, control-affine systems. We only consider systems with the same number of inputs as outputs. Such a system is sometimes called *square*. A general model for this class of systems has the form

$$\dot{x}(t) = f(x(t)) + \sum_{i=1}^{m} g_i(x(t))u_i(t) \tag{2.3a}$$

$$y(t) = h(x(t)) \tag{2.3b}$$

where $x \in \mathbb{R}^n$ is its state vector, $u \coloneqq \text{col}(u_1, \ldots, u_m) \in \mathbb{R}^m$ is its control input and, $y \in \mathbb{R}^m$ is the output. In this thesis the functions $f : \mathbb{R}^n \to \mathbb{R}^n$, $g_i, h : \mathbb{R}^n \to \mathbb{R}^m$ are always assumed smooth. For convenience the system can be written compactly as

$$\begin{aligned} \dot{x}(t) &= f(x(t)) + g(x(t))u(t) \\ y(t) &= h(x(t)) \end{aligned}$$

where $g : \mathbb{R}^n \to \mathbb{R}^{n\times m}$ is given by $g(x) = \begin{bmatrix} g_1(x) & \cdots & g_m(x) \end{bmatrix}$. An important special case of (2.3), and the main focus of this research, is the class of square L.T.I. systems with no feed through

$$\dot{x}(t) = Ax(t) + Bu(t) \tag{2.4a}$$

$$y(t) = Cx(t) \tag{2.4b}$$

where $A \in \mathbb{R}^{n\times n}$, $B \in \mathbb{R}^{n\times m}$ and $C \in \mathbb{R}^{m\times n}$ are constant matrices.

2.4 Partial Feedback Linearization

Feedback linearization is a technique used to control nonlinear systems of the form (2.3). When feasible, it allows control engineers to use standard L.T.I. control design techniques. In feedback linearization one seeks a specialized local coordinate transformation and feedback transformation, at a point in the state space, such that in the transformed coordinates the closed-loop system is (partially) linear, and the linear part of the dynamics is controllable.

2.4.1 Relative Degree

Intuitively, the relative degree of a system is the number of times one must differentiate the system output in order for the control input to appear. For S.I.S.O. L.T.I. systems, the relative degree equals the difference between the degree of the denominator and the numerator of the transfer function. To generalize to nonlinear M.I.M.O. systems of the form (2.3) care must be taken. In the M.I.M.O. case it is possible to have differentiated one of the system outputs only to have a subset of the control inputs appear. Different system outputs may also be dependent on different subsets of the input and may require different degrees of differentiation. In this thesis we do not consider such systems and only consider systems with uniform vector relative degree.

Definition 2.4.1. The system (2.3) is said to have **uniform vector relative degree** $\{r, \dots, r\}$ (m-times) at a point $x_0 \in \mathbb{R}^n$ if

$$\text{(i)}\ \ (\forall i \in \{0, 1, \dots, r-2\})(\exists \delta > 0)(\forall x \in B_\delta(x_0)) \begin{bmatrix} L_{g_1} L_f^i h(x) & \dots & L_{g_m} L_f^i h(x) \end{bmatrix} = 0,$$

(ii) $$\det \begin{bmatrix} L_{g_1} L_f^{r-1} h_1(x_0)) & \dots & L_{g_m} L_f^{r-1} h_1(x_0) \\ \vdots & & \vdots \\ L_{g_1} L_f^{r-1} h_m(x_0) & \dots & L_{g_m} L_f^{r-1} h_m(x_0) \end{bmatrix} \neq 0.$$

♦

The matrix in condition (ii) of Definition 2.4.1 is called the *decoupling matrix*. We will sometimes write it using compact notation as $L_g L_f^{r-1} h(x)$.

Specializing the above definition to the case of an L.T.I. system (2.4) we have that the triple (C, A, B) yields a uniform vector relative degree of $\{r, \dots, r\}$ if

$$(\forall j \in \{0, 1, \dots r-2\})\ CA^j B = 0$$

and $CA^{r-1}B$ is nonsingular. For linear systems, relative degree does not depend on the point x_0 at which the conditions are checked. The extent to which a nonlinear system can be transformed into a controllable linear system near a point x_0 is directly related to its relative degree at that point. We discuss this connection in the next section.

2.4.2 Byrnes-Isidori Normal Form

A system with uniform relative degree $\{r, \dots, r\}$ can be partially feedback linearized [17]. The controllable linear subsystem has dimension mr. If $mr = n$ then the nonlinear system (2.3) can be fully feedback linearized in a neighbourhood of x_0.

More specifically, if (2.3) has relative degree $\{r, \dots, r\}$ at x_0, then there exists an open set U containing x_0 and a map $T : U \subset \mathbb{R}^n \to \mathbb{R}^n$, which is a diffeomorphism onto its

image defined via

$$\begin{aligned} z_i &\coloneqq \phi_i(x), && (\forall\ i \in \mathbb{N}_{n-mr}) \\ q^i_j &\coloneqq L_f^{i-1} h_j(x), && (\forall\ i \in \mathbb{N}_r), \quad (\forall\ j \in \mathbb{N}_m). \end{aligned} \tag{2.5}$$

Here the state q^i_j is the $(i-1)$th derivative of the jth output. Let $q^i \coloneqq \operatorname{col}(q^i_1, \ldots, q^i_m) \in \mathbb{R}^m$ and let $q \coloneqq \operatorname{col}(q^1, \ldots, q^r)$. With these definitions, the q states represent the system output (2.3b) and its (Lie) derivatives. Let $z = \operatorname{col}(z_1, \ldots, z_{n-mr}) \in \mathbb{R}^{n-mr}$. The existence of the functions $\phi_i : U \to \mathbb{R}$ such that (2.5) is a valid diffeomorphism is guaranteed by [17, Proposition 5.1.2]. Practically, solving for the diffeomorphism may not be trivial.

If we express (2.3) in the (z, q)-dynamics defined above, the system reads

$$\begin{aligned} \dot{z} &= p(z, q) + r(z, q)u \\ \dot{q}^1 &= q^2 \\ &\cdots \\ \dot{q}^{r-1} &= q^r \\ \dot{q}^r &= L_f^r h(x) + \sum_{i=i}^{m} L_{g_i} L_f^{r-1} h(x) u_i = L_f^r h(x) + L_g L_f^{r-1} h(x) u \\ y &= q^1 \end{aligned} \tag{2.6}$$

where x should be expressed in terms of (z, q) using the inverse of T. In general no special structure can be imposed on the z-dynamics. The model (2.6) is the Byrnes-Isidori normal form for (2.3).

By definition of relative degree, the decoupling matrix $L_g L_f^{r-1} h$ is non-singular at $x = x_0$. Therefore, because f, g and h are all assumed smooth, it remains non-singular in a neighbourhood of x_0 which we take without loss of generality to be U. This means that

the state feedback controller

$$u = \left(L_g L_f^{r-1} h(x)\right)^{-1} \left(-L_f^r h(x) + v\right), \tag{2.7}$$

with $v = \mathrm{col}(v_1, \ldots, v_m)$ an auxiliary or outer-loop control signal, is well-defined in U. As a result, so long as the state of (2.3) remains in U, the system is feedback equivalent to

$$\begin{aligned}
\dot{z} &= p(z,q) + r(z,q)u \\
\dot{q}^1 &= q^2 \\
&\cdots \\
\dot{q}^{r-1} &= q^r \\
\dot{q}^r &= v \\
y &= q^1
\end{aligned}$$

The q-subsystem is easily seen to be linear and controllable and the input-output relationship between the input v and the output y is given in the Laplace domain by

$$Y(s) = \frac{1}{s^r} V(s).$$

When $mr = n$, there is no z-subsystem and the system (2.3) is feedback equivalent to a controllable linear system. When $mr < n$ the system is only partially linearized.

2.4.3 Invariance of Relative Degree under Output Transformations

Relative degree is a structural property of a system and invariant under coordinate transformations and feedback transformations [23]. The main result of this section is that the relative degree of a system at a point does not change when we apply a diffeomorphism to the output space. While such a fact may seem obvious, we are not aware of a proof of it and therefore we include a proof for completeness. We start with some preliminary results before proving the main result.

Proposition 2.4.2 (Scalar Vector Product Rule)**.** *If $f : \mathbb{R}^n \to \mathbb{R}^n$ and $\alpha : \mathbb{R}^n \to \mathbb{R}$ are differentiable functions, then*

$$\frac{\partial}{\partial x}\left(\alpha(x)f(x)\right) = \alpha(x)\frac{\partial(f(x))}{\partial x} + f(x)\frac{\partial(\alpha(x))}{\partial x}.$$

Proof. Direct calculations will be used to show the result. Let $f_i(x)$ denote the ith component function of f. Then using the usual product rule from vector calculus we have

$$\frac{\partial}{\partial x}\left(\alpha(x)f_i(x)\right) = \alpha(x)\frac{\partial(f_i(x))}{\partial x} + f_i(x)\frac{\partial(\alpha(x))}{\partial x}. \tag{2.8}$$

Apply (2.8) to each component of the vector $\alpha(x)f(x)$ to get the desired result. □

Proposition 2.4.3 (Matrix Vector Product Rule)**.** *If $f, h : \mathbb{R}^n \to \mathbb{R}^m$ and $M : \mathbb{R}^m \to \mathbb{R}^{m\times m}$ are differentiable functions, then*

$$\frac{\partial}{\partial x}\left(M(h(x))f(x)\right) = \left(\sum_{i=1}^{m} f_i(x)\left.\frac{\partial(M(y)e_i)}{\partial y}\right|_{y=h(x)}\right)\frac{\partial(h(x))}{\partial x} + M(h(x))\frac{\partial(f(x))}{\partial x}$$

where e_i is the ith natural basis vector of $\mathbb{R}^m$.

Proof. Once again, we prove the result by direct calculation. We have

$$\begin{aligned}\frac{\partial}{\partial x}\left(M(h(x))f(x)\right) &= \frac{\partial}{\partial x}\left(\sum_{i=1}^{m} f_i(x)M(h(x))e_i\right) \\ &= \sum_{i=1}^{m}\left(\frac{\partial}{\partial x}\left(f_i(x)M(h(x))e_i\right)\right).\end{aligned}$$

Now apply the results of Proposition 2.4.2 and the chain rule to each term in the above summation. For $i \in \{1, \ldots, m\}$ we have

$$\begin{aligned}\frac{\partial}{\partial x}\left(f_i(x)M(h(x))e_i\right) &= f_i(x)\frac{\partial(M(h(x))e_i)}{\partial x} + M(h(x))e_i\frac{\partial(f_i(x))}{\partial x} \\ &= f_i(x)\left.\frac{\partial(M(y)e_i)}{\partial y}\right|_{y=h(x)}\frac{\partial(h(x))}{\partial x} + M(h(x))e_i\frac{\partial(f_i(x))}{\partial x}.\end{aligned}$$

Substituting this expression into the summation above yields the desired result. □

Theorem 2.4.4. *Consider the nonlinear system (2.3) and let $T : U \subseteq \mathbb{R}^m \to \mathbb{R}^m$ be a diffeomorphism onto its image. For any $k \in \mathbb{N}$, there exist smooth functions $M_j^k : \mathbb{R}^{km} \to \mathbb{R}^{m\times m}$, $j \in \{0, \ldots, k-1\}$ such that*

$$L_f^k(T(h(x))) = \sum_{j=1}^{k-1} M_j^k(h(x), L_f h(x), \ldots, L_f^{k-1}h(x))L_f^j h(x) + \left.\frac{\partial(T(y))}{\partial x}\right|_{y=h(x)} L_f^k h(x). \quad (2.9)$$

Proof. We prove the proposition by induction. For the base case suppose $k = 1$. By the

chain rule

$$\begin{aligned} L_f(T(h(x))) &= \frac{\partial(T(h(x)))}{\partial x} f(x) \\ &= \left.\frac{\partial(T(y))}{\partial y}\right|_{y=h(x)} \frac{\partial(h(x))}{\partial x} f(x) \\ &= \left.\frac{\partial(T(y))}{\partial y}\right|_{y=h(x)} L_f h(x) \end{aligned}$$

showing that (2.9) holds for $k = 1$. Now assume (2.9) is true for some $k > 1$ and consider $L_f^{k+1} T(h(x))$. Proceeding

$$L_f^{k+1} T(h(x)) = \frac{\partial(L_f^k T(h(x)))}{\partial x} f(x). \tag{2.10}$$

By the induction hypothesis

$$L_f^k T(h(x)) = \sum_{j=1}^{k-1} M_j^k(h(x), L_f h(x), \ldots, L_f^{k-1} h(x)) L_f^j h(x) + \frac{\partial(T(h(x)))}{\partial x} L_f^k h(x).$$

By Proposition 2.4.3

$$\begin{aligned} \frac{\partial(M_j^k(h(x), L_f h(x), \ldots, L_f^{k-1} h(x)) L_f^j h(x))}{\partial x} = \\ \sum_{i=1}^{m} \sum_{p=0}^{k-1} \left((L_f^j h(x))_i \frac{\partial(M_j^k(h(x), L_f h(x), \ldots, L_f^{k-1} h(x)) e_i)}{\partial L_f^p h(x)} \frac{\partial(L_f^p h(x))}{\partial x} \right) \\ + M_j^k(h(x), \ldots, L_f^{k-1} h(x)) \frac{\partial(L_f^j h(x))}{\partial x} \end{aligned} \tag{2.11}$$

and

$$\frac{\partial}{\partial x}\left(\frac{\partial(T(h(x)))}{\partial x}L_f^k h(x)\right) = \left(\sum_{i=1}^{m}(L_f^k h(x))_i \frac{\partial}{\partial y}\left(\frac{\partial(T(y))}{\partial y}e_i\right)\Big|_{y=h(x)}\right)\frac{\partial(h(x))}{\partial x} + \frac{\partial(T(y))}{\partial y}\Big|_{y=h(x)}\frac{\partial(L_f^k h(x))}{\partial x}. \quad (2.12)$$

Therefore $\partial(L_f^k T(h(x)))/\partial x$ equals the sum of (2.11) and (2.12). Substituting this sum into (2.10) we obtain

$$\begin{aligned} L_f^{k+1}(T(h(x))) &= \sum_{j=1}^{k-1}\left(\sum_{i=1}^{m}\left[\sum_{p=0}^{k-1}\left((L_f^j h(x))_i \frac{\partial(M_j^k(h(x), L_f h(x), \ldots, L_f^{k-1}h(x))e_i)}{\partial L_f^p h(x)} L_f^{p+1}h(x)\right)\right]\right) \\ &+ \sum_{j=1}^{k-1} M_j^k(h(x), L_f h(x), \ldots, L_f^{k-1}h(x)) L_f^{j+1}h(x) \\ &+ \sum_{i=1}^{m}\left((L_f^k h(x))_i \frac{\partial}{\partial y}\left(\frac{\partial(T(y))}{\partial y}e_i\right)\Big|_{y=h(x)} L_f h(x)\right) + \frac{\partial(T(y))}{\partial y}\Big|_{y=h(x)} L_f^{k+1}h(x) \\ &=: \sum_{j=1}^{k} M_j^{k+1}(h(x), L_f h(x), \ldots, L_f^k h(x)) L_f^j h(x) + \frac{\partial(T(y))}{\partial y}\Big|_{y=h(x)} L_f^{k+1}h(x). \end{aligned}$$

□

Corollary 2.4.5. *Let $T : U \subseteq \mathbb{R}^m \to \mathbb{R}^m$ be a diffeomorphism onto its image. Then the system (2.3) has uniform vector relative degree $\{r, \ldots, r\}$ at $x_0 \in h^{-1}(U)$ if, and only if*

$$\begin{aligned} \dot{x}(t) &= f(x(t)) + g(x(t))u(t) \\ y(t) &= T \circ h(x(t)) \end{aligned} \quad (2.13)$$

has uniform vector relative degree of $\{r, \ldots, r\}$ at x_0.

Proof. Suppose that system (2.3) has uniform vector relative degree $\{r, \ldots, r\}$ at $x_0 \in$

$h^{-1}(U)$. We must show that the conditions of Definition 2.4.1 hold for (2.13) at x_0. For all $k \in \{0, \ldots, r-1\}$

$$L_g L_f^k (T(h(x))) = \frac{\partial (L_f^k T(h(x)))}{\partial x} g(x).$$

As shown in the proof of Theorem 2.4.4, the above differential equals the sum of (2.11) and (2.12). Therefore

$$L_g L_f^k T(h(x)) = \sum_{j=0}^{k-1} M_j^k (h(x), \ldots, L_f^k h(x)) L_g L_f^j h(x) + \frac{\partial (T(y))}{\partial y}\bigg|_{y=h(x)} L_g L_f^k h(x).$$

By condition (i) of Definition 2.4.1, for $k \in \{0, \ldots, r-2\}$, $L_g L_f^k h(x) = 0$ in a neighbourhood of x_0. Therefore we get that $L_g L_f^k T(h(x))$ also equals zero in a neighbourhood of x_0 for $k \in \{0, \ldots, r-2\}$. Similarly, for $k = r-1$ we get

$$L_g L_f^{r-1} T(h(x)) = \frac{\partial (T(y))}{\partial y}\bigg|_{y=h(x)} L_g L_f^{r-1} h(x).$$

Since $h(x_0) \in U$ and since T is a diffeomorphism onto its image, its Jacobian is non-singular at $h(x_0)$. Thus $L_g L_f^{r-1} T(h(x_0))$ is the product of nonsingular matrices and is therefore nonsingular.

Conversely, suppose that (2.13) has uniform vector relative degree $\{r, \ldots, r\}$ at $x_0 \in h^{-1}(U)$. Apply the output coordinate transformation $T^{-1} : T(U) \subseteq \mathbb{R}^m \to U \subseteq \mathbb{R}^m$ and repeat the same arguments as above with T^{-1} playing the role of T and $T \circ h$ playing the role of h.

□

2.5 Zero Dynamics of Linear Time-Invariant Systems

Following the construction from [17, 19, 26], we put a linear system with uniform vector relative degree into the Byrnes-Isidori normal form. This allows us to isolate its zero dynamics. Consider again a square linear time-invariant system

$$\begin{aligned} \dot{x}(t) &= A_p x(t) + B_p u_p(t) \\ y(t) &= C_p(t). \end{aligned} \tag{2.14}$$

Here we have added the subscript "p" to indicate plant and to distinguish the matrices (C_p, A_p, B_p) from those that follow in this discussion.

Suppose that system (2.14) has a uniform vector relative degree $\{r, \dots, r\}$. As discussed in Section 2.4.2, let $q = T_1 x \coloneqq (C_p x, C_p A_p x, \dots, C_p A_p^{r-1} x) \in \mathbb{R}^{rm}$ and select a matrix $T_0 \in \mathbb{R}^{(n-rm)\times n}$ whose rows span a subspace of the annihilator of $\operatorname{Im} B$ such that the $n \times n$ matrix

$$T \coloneqq \begin{bmatrix} T_0 \\ T_1 \end{bmatrix}$$

is nonsingular. Such a choice is always possible since T_1 is full rank [17, Lemma 5.1.1] and B is constant and therefore its columns define an involutive distribution [17, Proposition 5.1.2]. Additionally, see [18, Proposition 11.5.1] and [26], T_0 can be chosen such that defining $z \coloneqq T_0 x \in \mathbb{R}^{n-rm}$, in (z, q)-coordinates, system (2.4) reads

$$\begin{aligned} \dot{z} &= A_{00} z + A_{01} C q \\ \dot{q} &= \hat{A} q + \hat{B} \left(A_{10} z + A_{11} q + C_p A_p^{r-1} B_p u_p \right) \\ y &= \begin{bmatrix} 0 & C \end{bmatrix} \begin{bmatrix} z \\ q \end{bmatrix}. \end{aligned} \tag{2.15}$$

Denote the inverse of T as $x = M_0 z + M_1 q$ where M_0 and M_1 are partitions of T^{-1} defined implicitly by

$$\begin{bmatrix} M_0 & M_1 \end{bmatrix} \begin{bmatrix} T_0 \\ T_1 \end{bmatrix} = I_n.$$

Then the submatrices in (2.15) are given by

$$A_{00} = T_0 A_p M_0, \qquad A_{01} C = T_0 A_p M_1, \qquad A_{10} = C_p A_p^r M_0, \qquad A_{11} = C_p A_p^r M_1$$

and the triple $(\hat{C}, \hat{A}, \hat{B})$ is given by

$$\hat{A} = \begin{bmatrix} 0_m & I_m & 0_m & \cdot & \cdot & \cdot & 0_m \\ 0_m & 0_m & I_m & \cdot & \cdot & \cdot & 0_m \\ \cdot & \cdot & \cdot & \cdot & \cdot & \cdot & \cdot \\ 0_m & \cdot & \cdot & \cdot & \cdot & 0_m & I_m \\ 0_m & \cdot & \cdot & \cdot & \cdot & \cdot & 0_m \end{bmatrix} \in \mathbb{R}^{rm \times rm}, \qquad \hat{B} = \begin{bmatrix} 0_m \\ \cdot \\ \cdot \\ \cdot \\ 0_m \\ I_m \end{bmatrix} \in \mathbb{R}^{rm \times m} \tag{2.16}$$

and

$$\hat{C} = \begin{bmatrix} I_m & 0_m & \cdot & \cdot & \cdot & 0_m \end{bmatrix} \in \mathbb{R}^{m \times rm}.$$

The subspace

$$\mathcal{Z}^\star := \{(z, q) : q = 0\} = \operatorname{Im} \begin{bmatrix} I_{n-mr} \\ 0 \end{bmatrix} \tag{2.17}$$

is the zero dynamics manifold of (2.4) in (z, q)-coordinates. This manfold can be made invariant by applying the globally defined linear state feedback

$$u_p^\star = -(C_p A_p^{r-1} B_p)^{-1} (A_{10} z + A_{11} q).$$

With this controller, if the system is initialized on $\mathcal{Z}^\star$ then it remains there for all $t \geq 0$ and the corresponding output signal is identically equal to zero. The dynamics of (2.15) restricted to $\mathcal{Z}^\star$ are given by

$$\dot{z} = A_{00} z.$$

These are the zero dynamics of (2.15). Since the system (2.15) is obtained by a similarity transformation, it is easy to check that the transmission zeros (in the sense of [8]) of (2.15) are identical to those of (2.4) and are precisely the eigenvalues of the submatrix A_{00}.

Chapter 3

Path Following Normal Form for Linear Systems

Consider a linear, time-invariant, square plant with no feed through of the form

$$\dot{x}(t) = A_p x(t) + B_p u_p(t) \tag{3.1a}$$

$$y(t) = C_p x(t). \tag{3.1b}$$

assigned a closed curve, $\mathcal{C}$, in its output space. The plant is assumed to have uniform vector relative degree $\{r, \ldots, r\}$.

The essential idea of this section is to define a fictitious output for a linear system with a clear physical meaning for the path following control design problem. This output can be viewed as a coordinate change on the *output space* that results in a linear system with a *nonlinear* output instead of the original linear output. Then, if possible, one performs input-output feedback linearzation of the system with its redefined output. The resulting

(partially) feedback linearized system continues to have a useful physical interpretation in the context of path following and the resulting normal form greatly simplifies controller design. The costs associated with this simplification are that solutions are almost invariably local and susceptibility to poor performance from model uncertainty.

3.1 Class of Paths Considered

In this section, we describe the class of curves assigned to each agent which is identical to those in other works [9, 25]. The terms 'curve' and 'path' are used interchangeably throughout this work. We assume that each curve $\mathcal{C}$ is closed, has no self-intersections and has a smooth (C^∞) parameterization $\sigma : \mathbb{R} \to \mathbb{R}^m$ such that $\mathcal{C} = \mathrm{Im}(\sigma)$ and, for all $\lambda \in \mathbb{R}$, $\|\sigma'(\lambda)\| \neq 0$. We further assume, without loss of generality, that σ is unit speed parameterized, i.e., $\|\sigma'(\lambda)\| \equiv 1$. This is possible because σ is smooth and by assumption $\|\sigma'(\lambda)\| \neq 0$.

Under these assumptions, each curve σ is parameterized by its arc-length. The assumption of arc-length parametrized curves simplifies some of our subsequent analysis but the results contained within this thesis still remain valid even when this assumption does not hold.

Since $\mathcal{C}$ is closed, it has a finite length which we denote by $L > 0$ and the parameterization σ is L-periodic, i.e., $(\forall \lambda \in \mathbb{R})\ \sigma(\lambda + L) = \sigma(\lambda)$. In such cases, we take the domain of σ to be $\mathbb{T} = \mathbb{R}\,\mathrm{mod}L$ meaning the curve has the geometric structure of a circle, see Section 2.2.

Assumption 1 (Implicit Representation)**.** *There exists an open set U in $\mathbb{R}^m$ containing*

$\mathcal{C}$ and a smooth (C^∞) function $s : U \to \mathbb{R}^{m-1}$ that has zero as a regular value such that

$$\mathcal{C} = s^{-1}(0) = \{y \in U \subseteq \mathbb{R}^m : s(y) = 0\}. \tag{3.2}$$

◀

Let

$$\Gamma := \{x \in \mathbb{R}^n : C_p x \in \mathcal{C}\} = \{x \in \mathbb{R}^n : s(C_p x) = 0\} \tag{3.3}$$

denote the lift of the curve $\mathcal{C}$ to the state-space of (3.1). Since $\mathcal{C}$ is compact the following statements are equivalent:

(i) $y(t) \to \mathcal{C}$ as $t \to \infty$

(ii) $s(y(t)) \to 0$ as $t \to \infty$

(iii) $x(t) \to \Gamma$ as $t \to \infty$.

3.2 Path Following Outputs

As noted above, under Assumption 1, driving the output of (3.1) towards its path $\mathcal{C}$ can be viewed as an output stabilization problem for the output $s(y) = s(Cx)$. Intuitively, $\|s(y)\|$ can be viewed as a distance function from y to $\mathcal{C}$ and asymptotically driving this distance to zero solves the problem of making the output approach $\mathcal{C}$.

Following [7], let $\mathcal{N}(\mathcal{C}) \subset \mathbb{R}^m$ denote a tubular neighbourhood of the curve $\mathcal{C}$ characterized by the property that if $y \in \mathcal{N}(\mathcal{C})$, then there exists a unique $y^\star \in \mathcal{C}$ such that $\text{dist}(y, \mathcal{C}) := \inf_{p \in \mathcal{C}} \|y - p\| = \|y - y^\star\|$. Such a neighbourhood is guaranteed to exist since

$\mathcal{C}$ is, by the assumptions imposed in Section 3.1, an embedded submanifold of the output space $\mathbb{R}^m$. In fact, since $\mathcal{C}$ is compact, we can make the stronger statement that there exists an $\epsilon > 0$ such that

$$\{y \in \mathbb{R}^m : \text{dist}(y, \mathcal{C}) < \epsilon\} \subseteq \mathcal{N}(\mathcal{C}).$$

Introduce the projection

$$\begin{aligned} \varpi : \mathcal{N}(\mathcal{C}) \subset \mathbb{R}^m &\to \mathbb{T} \\ y &\mapsto \arg \inf_{\lambda \in \mathbb{T}} \|y - \sigma(\lambda)\|. \end{aligned} \tag{3.4}$$

The function (3.4) is as smooth as σ and returns the parameter $\lambda \in [0, L)$ which minimizes the distance from the output to the path, i.e., $\sigma(\varpi(y))$ is the point on the path closest to y.

The feasibility of computing this projection is dependent on the complexity of the curve. As λ belongs to a closed interval of the real line, one could exhaustively look through all possible values for the minimizing argument, $\lambda^* := \varpi(y)$. A more computationally efficient method could be to use the facts that: the inner product between two orthogonal vectors is zero and, the shortest distance from a point to a curve is always perpendicular to the curve (see Figure 3.1 below).

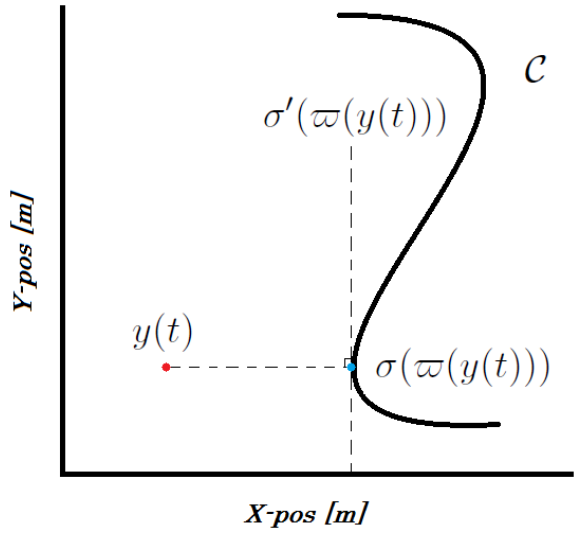

Figure 3.1: Schematic Diagram of Path Following Output $\varpi(y)$

With this in mind, we can search for λ^* by solving

$$\langle y - \sigma(\lambda^*),\ \sigma'(\lambda^*)\rangle = 0$$

using a well known root finding method such as the bisection, secant or Newton's method.

Combining the function $s : \mathbb{R}^m \to \mathbb{R}^{m-1}$ from (3.2) which implicitly defines the curve $\mathcal{C}$ via $\mathcal{C} = s^{-1}(0)$ with (3.4), we obtain a map

$$\begin{aligned} F_{\text{PF}} : U \subseteq \mathbb{R}^m &\to \mathbb{T} \times \mathbb{R}^{m-1} \\ y &\mapsto \begin{bmatrix} \varpi(y) \\ s(y) \end{bmatrix} \end{aligned} \tag{3.5}$$

whose domain is taken, without loss of generality, to be the neighbourhood U from Assumption 1.

Definition 3.2.1. The **path following output** of system (3.1) with respect to a closed curve $\mathcal{C}$ is

$$\begin{aligned} C_p^{-1}(U) \subseteq \mathbb{R}^n &\to \mathbb{T} \times \mathbb{R}^{m-1} \\ x &\mapsto F_{\mathrm{PF}} \circ C_p x. \end{aligned} \tag{3.6}$$

♦

We write $y_{\mathrm{PF}} = F_{\mathrm{PF}}(y) = F_{\mathrm{PF}} \circ C_p x =: h_{\mathrm{PF}}(x)$ to distinguish the path following output y_{PF} from the output y of (3.1b). The jth component of the path following output is denoted using an extra subscript, i.e., $h_{\mathrm{PF},j}(x)$. The differential of the path following output has a strong geometric interpretation as the next result shows.

Proposition 3.2.2 ([14, Lemma 3.1])**.** *For each $y \in \mathcal{C}$, the vector $\mathrm{d}\varpi_y$ is orthogonal to the rows of $\mathrm{d}s_y$.*

In light of Proposition 3.2.2, we are tempted to apply the classical inverse function theorem (Theorem 2.1.4) to the path following output and say it is a diffeomorphism. However, we must be careful because the codomain of the projection ϖ is $\mathbb{T} = \mathbb{R} \bmod L$ which is a smooth manifold, not a vector space. Therefore we need the inverse function theorem on manifolds. To state the theorem we first require some definitions.

Definition 3.2.3. Consider a function $F : M \to N$ where M and N are smooth manifolds. The function F is **smooth** if for every $p \in M$ there exist coordinate charts (U, φ) of M containing p and (V, ψ) containing $F(p)$, such that the expression of F in local coordinates $\hat{F} = \psi \circ F \circ \varphi^{-1}$ is smooth. ♦

Definition 3.2.4. Consider a function $F : M \to N$ where M and N are smooth manifolds. The function F is a **diffeomorphism** if it is bijective, smooth and its inverse $F^{-1} : N \to M$ is also smooth. Two manifolds M and N are **diffeomorphic** if there exists a diffeomorphism between them. ♦

More generally, a map between smooth manifolds $F : M \to N$ is called a local diffeomorphism at $p \in M$ if there exists an open set $U \subseteq M$ containing p such that $F : U \to F(U)$ is a diffeomorphism. If such a map is a local diffeomorphism at every p, then it is simply called a local diffeomorphism. The next result states that a necessary condition for a map between manifolds to be a local diffeomorphism at a point is that its differential be bijective.

Proposition 3.2.5. *Suppose that $F : M \to N$ is a diffeomorphism. Then its differential $\mathrm{d}F_p$ is an isomorphism at each $p \in M$.*

The proof of Proposition 3.2.5 can be found in Appendix A.

The inverse function theorem on manifolds can be used to determine if a map between manifolds is a local diffeomorphism at a given point. It states that the necessary condition from Proposition 3.2.5 is also sufficient.

Theorem 3.2.6 ([24, Theorem 7.10])**.** *Suppose M and N are smooth manifolds, $p \in M$ and $F : M \to N$ is a smooth map such that $\mathrm{d}F_p : T_pM \to T_{F(p)}N$ is bijective. Then there exists an open connected set U containing p such that $F : U \to F(U)$ is a diffeomorphism.*

Remark 3.2.7. The conditions of Theorem 3.2.6 can be checked as follows. Let $p \in M$ and let (U, φ) be a any smooth chart on M with $p \in U$. Let (V, ψ) be a smooth chart on N with $F(p) \in V$. Then $\mathrm{d}F_p$ is a bijection if, and only if the Jacobian matrix of its local representation $\mathrm{d}\hat{F}_{\varphi(p)}$ is a linear bijection, i.e., a non-singular square matrix. ◀

Together, Proposition 3.2.2 and Theorem 3.2.6 imply that (3.5) is a local diffeomorphism of system (3.1)'s output in a neighbourhood of each $y \in \mathcal{C}$. This however does not immediately mean that (3.5) maps an open set containing the path $\mathcal{C}$ diffeomorphically onto its image. To conclude this stronger property, we need a generalized version of Theorem 3.2.6 which requires the following preliminary result.

Proposition 3.2.8 ([13, Exercise 1.3.5]). *Let $F : M \to N$ be a local diffeomorphism. If F is one-to-one, then $F : M \to F(M)$ is a diffeomorphism.*

The proof of Proposition 3.2.8 can be found in Appendix A.

Theorem 3.2.9 ([13, Exercise 1.3.10]). *Let $F : M \to N$ be a smooth map that is one-to-one on a compact submanifold S of M. Suppose that for all $p \in S$*

$$\mathrm{d}F_p : T_pM \to T_{F(p)}N$$

is an isomorphism. Then F maps an open neighbourhood of S in M diffeomorphically onto an open neighbourhood of $F(S)$ in N.

The proof of Theorem 3.2.9 can be found in Appendix A.

With the above results in place, we can rigorously assert that the path following output maps an open set containing the assigned path $\mathcal{C}$ diffeomorphically into $\mathbb{T} \times \mathbb{R}^{m-1}$.

Corollary 3.2.10. *The function (3.5) maps an open neighbourhood of $\mathcal{C}$ in $\mathbb{R}^m$ diffeomorphically onto an open neighbourhood of $F_{\mathrm{PF}}(\mathcal{C})$ in $\mathbb{T} \times \mathbb{R}^{m-1}$.*

Proof. The result follows immediately from Proposition 3.2.2 and Theorem 3.2.9. □

3.3 Path Following Normal Form

When feasible, applying input-output feedback linearization to system (3.1) with respect to its path following output (3.6) yields a normal form which facilitates path following control design and, to some extent, analysis. The normal form has the useful property

of decomposing the system dynamics, as well as the control inputs, into those that are tangential and transversal to the given path.

We begin by showing that re-defining the output of (3.1) using the path following output (3.6) does not change its relative degree. Recall the definition of equation (3.3) for the lift, Γ, of the path into the state-space of (3.1). The set Γ is the set of all points in the state-space at which the corresponding output belongs to the curve $\mathcal{C}$. Note that, unlike $\mathcal{C}$, the set Γ is not compact.

Corollary 3.3.1. *System (3.1) with output (3.6) has a uniform vector relative degree of* $\{r, \dots, r\}$ *at each* $x \in \Gamma$.

Proof. By Corollary 2.4.5, a system's relative degree is invariant under output diffeomorphisms. By Corollary 3.2.10 the function (3.5) is a diffeomorphism in a neighbourhood of $\mathcal{C}$. Therefore, system (3.1) with output $F_{\mathrm{PF}} \circ C_p x$ has relative degree $\{r, \dots, r\}$ at each $C_p x \in \mathcal{C}$. □

The next two propositions are vital to constructing the path following normal form.

Proposition 3.3.2. *There exists an open set in* $\mathbb{R}^n$ *containing the lift (3.3) such that, at each point in the set, the* mr *differentials of* $L^{i-1}_{A_p x} h_{\mathrm{PF}}$, $i \in \mathbb{N}_r$, *are linearly independent.*

Proof. By Corollary 3.3.1 system (3.1) has vector relative degree $\{r, \dots, r\}$ at each point of Γ. Therefore, by [17, Lemma 5.1.1], the differentials of interest are linearly independent at each $x \in \Gamma$. By continuity of these differentials, they remain linearly independent in an open set containing Γ. □

Proposition 3.3.3. *At each* $\bar{x} \in \Gamma$, *there exist* $n - mr$ *independent linear functionals in the annihilator of* $\mathrm{Im}\,(B_p)$ *which are linearly independent of the differentials of* $L^{j-1}_{A_p x} h_{\mathrm{PF}}$, $j \in \mathbb{N}_r$.

Proof. Fix $\bar{x} \in \Gamma$. By [17, Proposition 5.1.2], noting that $\mathrm{Im}\,(B_p)$ can be viewed as a constant, and therefore an involutive distribution, it is always possible to select $n - mr$ functionals from the annihilator of $\mathrm{Im}\,(B_p)$ whose differentials are linearly independent from $\mathrm{d}L^{j-1}_{A_p x} h_{\mathrm{PF}}$, $j \in \mathbb{N}_r$, at $\bar{x}$. □

This shows that at each $\bar{x} \in \Gamma$, there exist $b_i' \in \mathrm{ann}\,(\mathrm{Im}\,(B))$, $i \in \mathbb{N}_{n-mr}$, such that, defining

$$\zeta_i \coloneqq b_i' x, \qquad i \in \mathbb{N}_{n-mr}, \tag{3.7a}$$

$$\eta_i \coloneqq L^{i-1}_{A_p x} h_{\mathrm{PF},1}(x), \qquad i \in \mathbb{N}_r, \tag{3.7b}$$

$$\xi_i^j \coloneqq L^{i-1}_{A_p x} h_{\mathrm{PF},j}(x), \qquad i \in \mathbb{N}_r, \quad j \in \{2, \dots, m\}, \tag{3.7c}$$

the map $x \mapsto (\zeta, \eta, \xi)$ is a local diffeomorphism at $\bar{x}$. Here $\zeta \coloneqq (\zeta_1, \dots, \zeta_{n-mr}) \in \mathbb{R}^{n-mr}$, $\eta \coloneqq (\eta_1, \eta_2 \dots, \eta_r) \in \mathbb{T} \times \mathbb{R}^{m-1}$, $\xi \coloneqq (\xi^2, \dots, \xi^m)$ with $\xi^j \coloneqq (\xi_1^j, \dots, \xi_r^j) \in \mathbb{R}^r$. The state ξ_i^j is the $(i-1)$th derivative of the jth path following output.

Therefore, there exists an open connected set $U_{\bar{x}} \subset \mathbb{R}^n$ containing $\bar{x} \in \Gamma$ where sys-

tem (3.1) expressed in (ζ, η, ξ)-coordinates reads

$$
\begin{aligned}
\dot{\zeta} &= q(\zeta, \eta, \xi) \\
\dot{\eta}_1 &= \eta_2 \\
&\cdots \\
\dot{\eta}_{r-1} &= \eta_r \\
\dot{\eta}_r &= L^r_{A_p x} h_{\mathrm{PF},1}(x) + L_{B_p} L^{r-1}_{A_p x} h_{\mathrm{PF},1} u_p \\
\dot{\xi}^2_1 &= \xi^2_2 \\
&\cdots \\
\dot{\xi}^2_{r-1} &= \xi^2_r \\
\dot{\xi}^2_r &= L^r_{A_p x} h_{\mathrm{PF},2}(x) + L_{B_p} L^{r-1}_{A_p x} h_{\mathrm{PF},2} u_p \\
\dot{\xi}^3_1 &= \xi^3_2 \\
&\cdots \\
\dot{\xi}^3_{r-1} &= \xi^3_r \\
\dot{\xi}^3_r &= L^r_{A_p x} h_{\mathrm{PF},3}(x) + L_{B_p} L^{r-1}_{A_p x} h_{\mathrm{PF},3} u_p \\
&\cdots \\
\dot{\xi}^m_1 &= \xi^m_2 \\
&\cdots \\
\dot{\xi}^m_{r-1} &= \xi^m_r \\
\dot{\xi}^m_r &= L^r_{A_p x} h_{\mathrm{PF},m}(x) + L_{B_p} L^{r-1}_{A_p x} h_{\mathrm{PF},m} u_p.
\end{aligned}
\tag{3.8}
$$

Of course we should express x in terms of (ζ, η, ξ) using the inverse of (3.7) so that the right-hand side of (3.8) is in terms of (ζ, η, ξ).

Definition 3.3.4. The **path following normal form** of an L.T.I. system (3.1) with relative degree $\{r, \ldots, r\}$ tasked with following a curve $\mathcal{C}$ satisfying the assumptions in Section 3.1 is given by (3.8). ♦

By Corollary 3.3.1, the $m \times m$ decoupling matrix $L_{B_p} L^{r-1}_{A_p x} h_{\mathrm{PF}}(x)$ is non-singular for all

$x \in U_{\bar{x}}$. This means that the feedback controller

$$u_p = (L_{B_p} L_{A_p x}^{r-1} h_{\mathrm{PF}}(x))^{-1} \left(-L_{A_p x}^{r} h_{\mathrm{PF}}(x) + \begin{bmatrix} v^{\parallel} \\ v_2^{\pitchfork} \\ \vdots \\ v_m^{\pitchfork} \end{bmatrix} \right), \tag{3.9}$$

where $v \coloneqq \mathrm{col}(v^{\parallel}, v_2^{\pitchfork}, \ldots, v_m^{\pitchfork})$ is an auxiliary control input, is well-defined for all $x \in U_{\bar{x}}$ and therefore system (3.1) is feedback equivalent to

$$\begin{aligned}
\dot{\zeta} &= q(\zeta, \eta, \xi) \\
\dot{\eta}_1 &= \eta_2 \\
&\cdots \\
\dot{\eta}_{r-1} &= \eta_r \\
\dot{\eta}_r &= v^{\parallel} \\
\dot{\xi}_1^2 &= \xi_2^2 \\
&\cdots \\
\dot{\xi}_{r-1}^2 &= \xi_r^2 \\
\dot{\xi}_r^2 &= v_2^{\pitchfork} \\
\dot{\xi}_1^3 &= \xi_2^3 \\
&\cdots \\
\dot{\xi}_{r-1}^3 &= \xi_r^3 \\
\dot{\xi}_r^3 &= v_3^{\pitchfork} \\
&\cdots \\
\dot{\xi}_1^m &= \xi_2^m \\
&\cdots \\
\dot{\xi}_{r-1}^m &= \xi_r^m \\
\dot{\xi}_r^m &= v_m^{\pitchfork}
\end{aligned} \tag{3.10}$$

for all $x \in U_{\bar{x}}$. If we define the matrices

$$A \coloneqq \begin{bmatrix} 0 & 1 & 0 & \cdot & \cdot & \cdot & 0 \\ 0 & 0 & 1 & \cdot & \cdot & \cdot & 0 \\ \cdot & \cdot & \cdot & \cdot & \cdot & \cdot & \cdot \\ 0 & \cdot & \cdot & \cdot & \cdot & 0 & 1 \\ 0 & \cdot & \cdot & \cdot & \cdot & \cdot & 0 \end{bmatrix} \in \mathbb{R}^{r \times r}, \qquad b = \begin{bmatrix} 0 \\ \cdot \\ \cdot \\ \cdot \\ 0 \\ 1 \end{bmatrix} \in \mathbb{R}^r \tag{3.11}$$

then (3.10) can be compactly written

$$\begin{aligned} \dot{\zeta} &= q(\zeta, \eta, \xi) \\ \dot{\eta} &= A\eta + bv^{\parallel} \\ \dot{\xi}^2 &= A\xi^2 + bv_2^{\pitchfork} \\ \dot{\xi}^3 &= A\xi^3 + bv_3^{\pitchfork} \\ &\cdots \\ \dot{\xi}^m &= A\xi^m + bv_m^{\pitchfork}. \end{aligned} \tag{3.12}$$

Or, if we define

$$\mathbf{A} \coloneqq \operatorname{diag}(\underbrace{A, \ldots, A}_{m-1 \text{ times}}), \qquad \mathbf{B} \coloneqq \operatorname{diag}(\underbrace{b, \ldots, b}_{m-1 \text{ times}}), \qquad v^{\pitchfork} \coloneqq (v_2^{\pitchfork}, \ldots, v_m^{\pitchfork}) \tag{3.13}$$

even more compactly as

$$\begin{aligned} \dot{\zeta} &= q(\zeta, \eta, \xi) \\ \dot{\eta} &= A\eta + bv^{\parallel} \\ \dot{\xi} &= \mathbf{A}\xi + \mathbf{B}v^{\pitchfork}. \end{aligned} \tag{3.14}$$

The path following output is given by

$$y_{\mathrm{PF}} = \begin{bmatrix} \eta_1 \\ \xi^2 \end{bmatrix}. \tag{3.15}$$

We choose to keep the η- and ξ-subsystems separate in (3.14) because they have different physical meanings in the context of path following. The ξ-subsystem determines the motion towards the path and regulating it to zero has the practical interpretation of the system output belonging to the desired path. The η-subsystem determines the motion along the path. This connection is exploited in Proposition 4.1.1. The ζ-dynamics represent dynamics that have no discernable effect on the path following output. They are the internal dynamics of the system and are closely related to the zero dynamics of the original system (3.1).

We are tempted to argue that system (3.1) is feedback equivalent to (3.14) in a neighbourhood of the *entire* set Γ. However, it is not immediately clear that this is the case because of our special choice of ζ-states and because the term $L^r_{A_p x} h_{\mathrm{PF}}(x)$ in the feedback (3.9) may not be bounded over all of Γ since Γ is not a bounded set. What is true, by [18, Proposition 11.5.1], is that there exists a diffeomorphism between an open set containing Γ onto its image in which system (3.1) is differentially equivalent to the path following normal form (3.8) with the difference being that the ζ-dynamics are replaced with a differential equation of form

$$\zeta = q(\zeta, \eta, \xi) + p(\zeta, \eta, \xi) u_p.$$

3.4 Relationship Between Internal & Zero Dynamics

At this point, for clarity of exposition, it is convenient to work with system (3.1) in (z, q)-coordinates (2.15). The system with path following output reads

$$\begin{aligned}\dot{z} &= A_{00}z + A_{01}Cq \\ \dot{q} &= \hat{A}q + \hat{B}\left(A_{10}z + A_{11}q + C_pA_p^{r-1}B_pu_p\right) \\ y_{\mathrm{PF}} &= F_{\mathrm{PF}}(Cq).\end{aligned}$$

We immediately see from the definitions of the states η (eqn. (3.7b)) and ξ (eqn. (3.7c)) and from the definition of the matrices $\hat{A}$ and $\hat{B}$ (eqn. (2.16)), that in (z, q)-coordinates the (η, ξ)-states only depend on the q states in (2.15). Let

$$\zeta_i = z_i, \qquad i \in \mathbb{N}_{n-mr}, \tag{3.16a}$$

$$\eta_i \coloneqq L_{\hat{A}q}^{i-1}h_{\mathrm{PF},1}(q), \qquad i \in \mathbb{N}_r, \tag{3.16b}$$

$$\xi_i^j \coloneqq L_{\hat{A}q}^{i-1}h_{\mathrm{PF},j}(q), \qquad i \in \mathbb{N}_r, \quad j \in \{2, \dots, m\} \tag{3.16c}$$

Proposition 3.4.1. *The mapping defined by (3.16) maps an open subset of $\mathbb{R}^n$ containing the set*

$$\Gamma_\star \coloneqq \left\{(z, q) \in \mathbb{R}^{n-mr} \times \mathbb{R}^{mr} : Cq \in \mathcal{C}, C\hat{A}q = \cdots C\hat{A}^{r-1}q = 0\right\} \tag{3.17}$$

diffeomorphically onto its image.

To prove this result we need an even more general version of the inverse function theorem.

Theorem 3.4.2 ([13, Exercise 1.8.14])**.** *Suppose that $F : M \to N$ is map between manifolds. Let $S \subset M$ be a submanifold of M. If*

(i) for all $p \in S$, $\mathrm{d}F_p$ is an isomorphism, and

(ii) F maps S diffeomorphically onto $F(S)$,

then F maps a neighbourhood of S diffeomorphically onto a neighbourhood of $F(S)$.

The proof of Theorem 3.4.2 can be found in Appendix A.

Proof of Proposition 3.4.1. We prove the result by showing that the conditions of Theorem 3.4.2 hold.

Since (a) relative degree is invariant under similarity transformations, (b) the map from $(z, q) \mapsto (\eta, \xi)$ in (3.16) is independent of z, and (c) the definition (3.16a) of the ζ states, we have by Proposition 3.3.2 and the fact that $\Gamma_\star \subset \Gamma$, that the differential of the map from $(q, z) \mapsto (\zeta, \eta, \xi)$ is an isomorphism at each point on $\Gamma_\star$.

By Theorem 2.4.4 and Equations (3.16b), (3.16c), we have that the image of $\Gamma_\star$ under the map (3.16) is

$$\begin{aligned}
\zeta &= z, \\
\eta_1 &= \varpi(Cq), \\
\eta_2 &= \cdots = \eta_r = 0 \\
\xi^2 &= \cdots = \xi^m = 0.
\end{aligned}$$

The inverse on the above set is

$$\begin{aligned}
z &= \zeta \\
(q_1, \ldots, q_m) &= \sigma(\eta_1) \\
(q_{m+1}, \ldots, q_{mr}) &= (0, \ldots, 0)
\end{aligned}$$

The existence of this inverse shows that (3.16) maps $\Gamma_\star$ diffeomorphically onto its image. Therefore, having shown that conditions (i) and (ii) of Theorem 3.4.2 hold, we are done. □

Remark 3.4.3. Employing the analysis from Section 2.2, we see that the set (3.17) is diffeomorphic to $\mathbb{T} \times \mathbb{R}^{n-mr}$. The set can also be expressed in x-coordinates as

$$\Gamma_\star \coloneqq \left\{ x \in \mathbb{R}^n : C_p x \in \mathcal{C},\ C_p A_p x = \cdots = C_p A_p^{r-1} x = 0 \right\}. \tag{3.18}$$

We can interpret $\Gamma_\star$ as all those points in the state-space of (3.1) for which the output is constant and on the assigned path. ◀

Remark 3.4.4. The dimension of the zero dynamics subspace (2.17) of (2.15) is one less than the dimension of (3.17). The difference is that on the zero dynamics manifold (2.17) the system output is constrained to be constant and equal to zero while on the path following manifold (3.17) the system output is constant but can be located at any point on the assigned path $\mathcal{C}$. ◀

Let $T : U \subset \mathbb{R}^n \to T(U)$ denote the coordinate transformation defined by (3.16). By Proposition 3.4.1, the path following normal form of (2.15) (equivalently system (3.1)), valid in an open set containing (3.17), is given by

$$
\begin{aligned}
\dot{\zeta} &= A_{00}\zeta + A_{01}F_{\mathrm{PF}}^{-1}(y_{\mathrm{PF}}) \\
\dot{\eta}_1 &= \eta_2 \\
&\cdots \\
\dot{\eta}_{r-1} &= \eta_r \\
\dot{\eta}_r &= a_1(\zeta, q) + b_1(q)u_p \\
\dot{\xi}_1^2 &= \xi_2^2 \\
&\cdots \\
\dot{\xi}_{r-1}^2 &= \xi_r^2 \\
\dot{\xi}_r^2 &= a_2(\zeta, q) + b_2(q)u_p \\
\dot{\xi}_1^3 &= \xi_2^3 \\
&\cdots \\
\dot{\xi}_{r-1}^3 &= \xi_r^3 \\
\dot{\xi}_r^3 &= a_3(\zeta, q) + b_3(q)u_p \\
&\cdots \\
\dot{\xi}_1^m &= \xi_2^m \\
&\cdots \\
\dot{\xi}_{r-1}^m &= \xi_r^m \\
\dot{\xi}_r^m &= a_m(\zeta, q) + b_m(q)u_p \\
y_{\mathrm{PF}} &= \begin{bmatrix} \eta_1 \\ \xi^2 \end{bmatrix}.
\end{aligned}
\tag{3.19}
$$

Of course we should express q in terms of η and ξ using $T^{-1}(\zeta, \eta, \xi)$ so that the right-hand side of (3.19) is in terms of (ζ, η, ξ). We emphasize that this is a *global normal form* valid not just in a neighbourhood of a point, but rather in a neighbourhood of the entire

set (3.17). Grouping the terms in which the control input u_p appears we have

$$\begin{bmatrix} \dot{\eta}_r \\ \dot{\xi}_r^2 \\ \dot{\xi}_r^3 \\ \dots \\ \dot{\xi}_r^m \end{bmatrix} = \begin{bmatrix} a_1(\zeta, q) \\ a_2(\zeta, q) \\ a_3(\zeta, q) \\ \dots \\ a_m(\zeta, q) \end{bmatrix} + \begin{bmatrix} b_1(q) \\ b_2(q) \\ b_3(q) \\ \dots \\ b_m(q) \end{bmatrix} u_p$$
$$\coloneqq \mathrm{d}L_{\hat{A}q}^{r-1} h_{\mathrm{PF}}(q) \hat{B} \left(A_{10}\zeta + A_{11} q \right) + \mathrm{d}L_{\hat{A}q}^{r-1} h_{\mathrm{PF}}(q) \hat{B} C_p A_p^{r-1} B_p u_p.$$

We can simplify this expression further using Theorem 2.4.4 to note that

$$\mathrm{d}L_{\hat{A}q}^{r-1} h_{\mathrm{PF}}(q) \hat{B} = \mathrm{d}F_{\mathrm{PF}}|_{Cq}.$$

Therefore we can write

$$\begin{bmatrix} \dot{\eta}_r \\ \dot{\xi}_r^2 \\ \dot{\xi}_r^3 \\ \dots \\ \dot{\xi}_r^m \end{bmatrix} = A(\zeta, q) + B(q) u_p \coloneqq \mathrm{d}F_{\mathrm{PF}}|_{Cq} \left(A_{10}\zeta + A_{11} q \right) + \mathrm{d}F_{\mathrm{PF}}|_{Cq} C_p A_p^{r-1} B_p u_p.$$

Since (3.1) is assumed to have relative degree $\{r, \dots, r\}$ and since F_{PF} is a diffeomorphism, Corollary 2.4.5 implies that the $m \times m$ matrix $B(q)$ is non-singular at every point of $\Gamma_\star$. Therefore,

$$\inf_{(z,q) \in \Gamma_\star} \det B(q) = \min_{Cq \in \mathcal{C}} \det \left(\mathrm{d}F_{\mathrm{PF}}|_{Cq} C_p A_p^{r-1} B_p \right) = \det \left(C_p A_p^{r-1} B_p \right) \min_{Cq \in \mathcal{C}} \det \left(\mathrm{d}F_{\mathrm{PF}}|_{Cq} \right) > 0.$$

Here we use the fact that $\mathcal{C}$ is a compact set. Therefore, the matrix $B(q)$ is globally invertible in a neighbourhood of $\Gamma_\star$. The feedback controller

$$u_p = B^{-1}(q)\left(-A(\zeta, q) + \begin{bmatrix} v^{\parallel} \\ v^{\pitchfork} \end{bmatrix}\right)$$

is well-defined in a neighbourhood of $\Gamma_\star$ and, if we set $v^{\pitchfork} = 0$, $v^{\parallel} = 0$, the feedback makes $\Gamma_\star$ invariant for the controlled system. The dynamics of the system restricted to (3.17) become

$$\dot{\zeta} = A_{00}\zeta + A_{01}\sigma(\eta_1)$$

where η_1 is a constant determined by where on the path the system lies. This constant equals $\varpi(Cq) = \varpi(C_p x)$.

If we allow the system to move along its assigned path, then the dynamics of the system restricted to the path, i.e., with $\xi = 0$ become

$$\begin{aligned} \dot{\zeta} &= A_{00}\zeta + A_{01}\sigma(\eta_1) \\ \dot{\eta}_1 &= \eta_2 \\ &\cdots \\ \dot{\eta}_{r-1} &= \eta_r \\ \dot{\eta}_r &= v^{\parallel}. \end{aligned}$$

Of course since the set $\Gamma_\star$ is unbounded, the term $A(\zeta, q)$ may be unbounded because $\|\zeta(t)\|$ may be undounded. As a result, in practice, it may not be possible to enforce invariance of $\Gamma_\star$ nor the path for all $t \geq 0$ due to actuator saturation. If the system is minimum phase, then A_{00} is Hurwitz and boundedness of the path ensures that the ζ dynamics are

bounded.

Example 3.4.1. (Double mass system) We now provide an illustrative example based on the system from [2] to demonstrate the constructions discussed. We use a double mass system wherein a small mass m lays atop a driven vehicle with mass M in the plane. The system can be modeled using the dynamic equations

$$M\ddot{y} = D(\dot{z} - \dot{y}) + u, \qquad m\ddot{z} = D(\dot{y} - \dot{z}) + G(z - y),$$

where $D, G \in \mathbb{R}^{2\times 2}$ are diagonal matrices with strictly positive diagonal elements, $u \in \mathbb{R}^2$ is the force and $y, z \in \mathbb{R}^2$ are the (x, y)-positions of the vehicle and mass in the plane, respectively. The position of the larger mass y in the plane is taken as the system output. The curve $\mathcal{C}$ in the output space is taken to be a circle of unit radius centered at the origin.

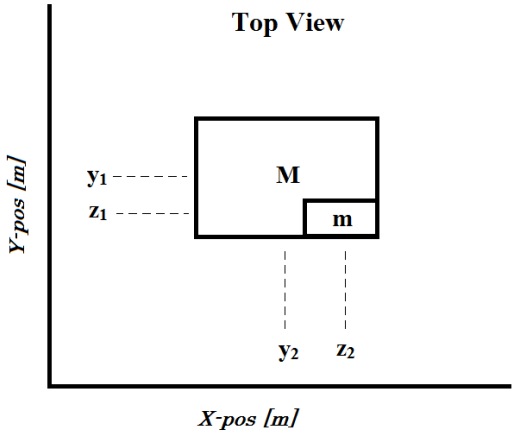

(a) Top View

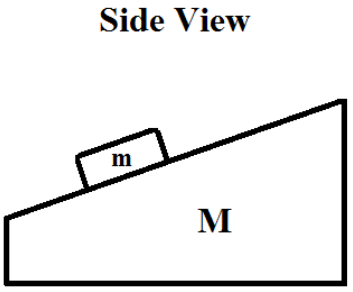

(b) Side View

Figure 3.2: Double Mass System

It is easily checked through direct calculations of the conditions in Definition 2.4.1 that the system yields a well-defined relative degree $\{2, 2\}$. Placing the double mass system into

the path following normal form is accomplished in the following way. First define the state vector $x = [z_1, \dot{z}_1, z_2, \dot{z}_2, y_1, \dot{y}_1, y_2, \dot{y}_2]^\top$ and it's corresponding triple (C_p, A_p, B_p) describing the dynamics of the system. The system output is $y = \mathrm{col}(y_1, y_2)$. We define our implicit representation of the curve as the zero level set of the unit circle, $s(y) = y_1^2 + y_2^2 - 1$. For a circle, the projection from the system output to the closest point on the path may be taken as $\varpi(y) = \mathrm{atan2}(y_2, y_1)$, where atan2 is the four quadrant arctangent function with codomain $(-\pi, \pi]$. We use these to redefine the output of the system to the path following outputs.

Converting this system to the path following normal form (3.14), we get that the diffeomorphism $x \mapsto (\zeta, \eta, \xi)$ is defined via

$$\begin{bmatrix} \zeta_1 \\ \zeta_2 \\ \zeta_3 \\ \zeta_4 \\ \eta_1 \\ \eta_2 \\ \xi_1^2 \\ \xi_2^2 \end{bmatrix} = \begin{bmatrix} x_1 \\ x_2 \\ x_3 \\ x_4 \\ \mathrm{atan2}\left(x_7, x_5\right) \\ \mathrm{d}\varpi_y C(Ax + Bu) \\ x_5^2 + x_7^2 - 1 \\ \mathrm{d}s_y C(Ax + Bu) \end{bmatrix}$$

with system dynamics

$$\begin{bmatrix} \dot{\zeta}_1 \\ \dot{\zeta}_2 \\ \\ \dot{\zeta}_3 \\ \dot{\zeta}_4 \\ \\ \dot{\eta}_1 \\ \dot{\eta}_2 \\ \dot{\xi}_1^2 \\ \dot{\xi}_2^2 \end{bmatrix} = \begin{bmatrix} \zeta_2 \\ \frac{D_{1,1}}{m}\left[\left(\frac{\xi_2^2}{2\sqrt{\xi_1^2+R^2}}\cos(\frac{2\pi}{L}\eta_1) - \frac{2\pi}{L}\eta_2\sqrt{\xi_1^2+R^2}\sin(\frac{2\pi}{L}\eta_1)\right) - \zeta_2\right] \\ \quad + \frac{G_{1,1}}{m}\left(\zeta_1 - \sqrt{\xi_1^2+R^2}\cos(\frac{2\pi}{L}\eta_1)\right) \\ \zeta_4 \\ \frac{D_{2,2}}{m}\left[\left(\frac{\xi_2^2}{2\sqrt{\xi_1^2+R^2}}\sin(\frac{2\pi}{L}\eta_1) + \frac{2\pi}{L}\eta_2\sqrt{\xi_1^2+R^2}\cos(\frac{2\pi}{L}\eta_1)\right) - \zeta_4\right] \\ \quad + \frac{G_{2,2}}{m}\left(\zeta_3 - \sqrt{\xi_1^2+R^2}\cos(\frac{2\pi}{L}\eta_1)\right) \\ \eta_2 \\ L_{Ax}^2 s(y) + [L_{B_1}L_{Ax}s(y), L_{B_2}L_{Ax}s(y)]u \\ \xi_2^2 \\ L_{Ax}^2 \varpi(y) + [L_{B_1}L_{Ax}\varpi(y), L_{B_2}L_{Ax}\varpi(y)]u \end{bmatrix}$$

$$y_{\text{PF}} = \begin{bmatrix} \eta_1 \\ \xi_1^2 \end{bmatrix},$$

where B_i is the ith column of B_p. We may now use the control input (3.9) to facilitate

partial feedback linearizion

$$\begin{bmatrix} \dot{\zeta}_1 \\ \dot{\zeta}_2 \\ \\ \dot{\zeta}_3 \\ \dot{\zeta}_4 \\ \\ \dot{\eta}_1 \\ \dot{\eta}_2 \\ \dot{\xi}_1^2 \\ \dot{\xi}_2^2 \end{bmatrix} = \begin{bmatrix} \zeta_2 \\ \frac{D_{1,1}}{m}\left[\left(\frac{\xi_2^2}{2\sqrt{\xi_1^2+R^2}}\cos(\frac{2\pi}{L}\eta_1) - \frac{2\pi}{L}\eta_2\sqrt{\xi_1^2+R^2}\sin(\frac{2\pi}{L}\eta_1)\right) - \zeta_2\right] \\ \qquad + \frac{G_{1,1}}{m}\left(\zeta_1 - \sqrt{\xi_1^2+R^2}\cos(\frac{2\pi}{L}\eta_1)\right) \\ \zeta_4 \\ \frac{D_{2,2}}{m}\left[\left(\frac{\xi_2^2}{2\sqrt{\xi_1^2+R^2}}\sin(\frac{2\pi}{L}\eta_1) + \frac{2\pi}{L}\eta_2\sqrt{\xi_1^2+R^2}\cos(\frac{2\pi}{L}\eta_1)\right) - \zeta_4\right] \\ \qquad + \frac{G_{2,2}}{m}\left(\zeta_3 - \sqrt{\xi_1^2+R^2}\cos(\frac{2\pi}{L}\eta_1)\right) \\ \eta_2 \\ v^{\parallel} \\ \xi_2^2 \\ v^{\pitchfork} \end{bmatrix}.$$

Now $v^{\pitchfork}$ can be designed to make $\xi \to 0$ as $t \to \infty$ and have the system output approach the designated curve. This is done independently from designing $v^{\parallel}$ for where on the unit circle the double mass system should be. $\triangle$

Chapter 4

Path Following for Linear Time Invariant Systems

In this chapter, we solve a path following problem for a linear time-invariant system assigned a closed path in its output space. At its core, the problem is to design a feedback controller such that the system output approaches its specified path. The controller should make the path invariant and should track a desired motion along the path.

4.1 Problem Statement

Consider a single linear, time-invariant, square plant with no feed through of the form:

$$\dot{x}(t) = A_p x(t) + B_p u_p(t) \tag{4.1a}$$

$$y(t) = C_p x(t). \tag{4.1b}$$

The pair (A_p, B_p) is assumed to be controllable and the triple (C_p, A_p, B_p) has vector relative degree $\{r, \ldots, r\}$. The plant is assigned a closed curve $\mathcal{C}$ in its output space satisfying all the assumptions of Section 3.1. We are also given a desired motion along the curve expressed in terms of an exosystem.

Assumption 2 (Exosystem)**.** *The desired motion along the assigned curve $\mathcal{C}$ is generated as the output of a system of the form*

$$\begin{aligned} \frac{\mathrm{d}}{\mathrm{d}t} w(\theta(t)) &= \frac{\mathrm{d}\theta}{\mathrm{d}t} S w(\theta(t)), \qquad w(\theta(0)) = w_0 \\ r(\theta(t)) &= \sigma(Q w(\theta(t))) \end{aligned} \tag{4.2}$$

where $\sigma(S) \subset \mathbb{C}^- \cup j\mathbb{R}$, $Q \in \mathbb{R}^{1 \times \dim(w)}$ and $\theta : [0, \infty) \to \mathbb{R}$ is piecewise smooth.

Since the exosystem in Assumption 2 produces a reference for a system's motion along the path, the *timing law* [26] θ may be interpreted as a path parameter which re-parameterizes the desired motion along the path. The evolution of θ can be used to further control the motion along the path. Setting $\theta(t) = t$ results in the usual trajectory tracking framework. In this manner, the path following control design problem can be viewed as a tracking problem. In the first part of this chapter, we assume that θ is given while in the second part, we use the freedom to select the timing law.

Our objective is to design a full information feedback controller such that:

(i) $y \to r(\theta(t))$ as $t \to \infty$ for all initial conditions in a neighbourhood of the path.

(ii) The path is invariant in the sense that if $y(0) \in \mathcal{C}$ and the system's initial motion is sufficiently tangent to the path, then $y(t) \in \mathcal{C}$ for all $t \geq 0$ even when $y(0) \neq r(\theta(0))$.

(iii) The system's state is bounded for all time.

4.1.1 Translation to Path Following Outputs

The utility of using the path following output (3.6) and the path following normal form (3.19) for path following control design lies in the fact that regulating the last $m-1$ components of y_{PF} to zero implies that the system output is approaching $\mathcal{C}$. The first component of y_{PF} determines the point on the curve closest to the actual system output (3.1b).

Proposition 4.1.1. *Consider system (3.1) assigned a curve $\mathcal{C}$ in its output space and a desired motion along the curve given by (4.2). Then $y(t) = r(\theta(t))$ if, and only if*

$$y_{\text{PF}}(t) = \begin{bmatrix} \operatorname{mod}(Qw(\theta(t)), L) \\ 0 \\ \vdots \\ 0 \end{bmatrix}$$

Proof. Let $t \geq 0$ be arbitrary and suppose that $y(t) = r(\theta(t))$. Then $y(t) \in \mathcal{C}$ which means that $s(y(t)) = 0$ and therefore the last $m-1$ components of $y_{\text{PF}}(t)$ equal zero. Furthermore, by definition of the function ϖ

$$\sigma(\varpi(y(t))) = y(t) = \sigma(Qw(\theta(t))).$$

Therefore, since σ is L-periodic,

$$\varpi(y(t)) = \operatorname{mod}(Qw(\theta(t)), L)$$

Conversely, suppose that $y_{\text{PF}}(t)$ equals $(\operatorname{mod}(Qw(\theta(t)), L), 0, \ldots, 0)$. Then $s(y(t)) = 0$ which implies $y(t) \in s^{-1}(0) = \mathcal{C}$. Since $y(t) \in \mathcal{C}$, we again have that $\sigma(\varpi(y(t))) = y(t)$. But $\varpi(y(t)) = \operatorname{mod}(Qw(\theta(t)), L)$ by assumption and therfore, using the L-periodicity of

the parameterization σ,

$$y(t) = \sigma(\mathrm{mod}(Qw(\theta(t)), L)) = \sigma(Qw(\theta(t)))$$

□

The requirements of the problem statement may now be expressed in terms of the path following outputs instead. Our objective is to design a full information feedback controller such that:

(i) $y_{\mathrm{PF}} \to \mathrm{col}(\mathrm{mod}(Qw(\theta(t)), L), 0, \ldots, 0)$ as $t \to \infty$.

(ii) If $\xi(0) = 0$, then $\xi(t) = 0$ for all $t \geq 0$.

(iii) $\|\zeta\|$ is bounded.

4.2 Solution for Minimum Phase Systems

In this section we make the following assumption.

Assumption 3 (Minimum Phase)**.** *All the transmission zeros of the system* (4.1) *have negative real parts.*

Assumption 3 means that for all $\lambda \in \mathbb{C}^-$,

$$\mathrm{rank}\left(\begin{bmatrix} A_p - \lambda I_n & B_p \\ C_p & 0 \end{bmatrix}\right) = n + m.$$

It also means that the matrix A_{00} in the normal forms (2.15) and (3.19) is Hurwitz.

In light of Proposition 4.1.1, we would like to make η_1 approach $\operatorname{mod}(Qw(\theta(t)), L)$. To measure the error between the variable $\eta_1 \in \mathbb{T}$ and $\operatorname{mod}(Qw(\theta(t)), L) \in \mathbb{T}$, we use the ideas from Section 2.2 to define the tracking error.

Definition 4.2.1. For any exosystem of the form (4.2), the **arc-error** is

$$e_{\text{arc}} \coloneqq \frac{L}{2\pi} \text{dist}_{\mathbb{S}} \left(\exp\left(j \frac{2\pi}{L} \eta_1 \right), \exp\left(j \frac{2\pi}{L} \operatorname{mod}\left(Qw(\theta(t)), L \right) \right) \right). \tag{4.3}$$

♦

We first map variables on $\mathbb{T}$ to points on the unit circle $\mathbb{S}$. We then compute the signed distance between these points on the circle and then normalize to an arc-length between $(-L/2, L/2]$.

Define, for $i \in \mathbb{N}_r$, the tangential tracking errors

$$e_i(t) \coloneqq \frac{\mathrm{d}^{i-1}}{\mathrm{d}t^{i-1}} \left(\eta_i(t) - \operatorname{mod}(Qw(\theta(t)), L) \right). \tag{4.4}$$

With this definition we have that $e_{\text{arc}} = \frac{L}{2\pi} \arg\left(\exp\left(j \frac{2\pi}{L} e_1 \right) \right)$ and, applying the chain rule gives that $\dot{e}_{\text{arc}}(t) = \dot{e}_1(t)$. A proof of this statement can be found in Appendix A. Define the vector $\mathbf{e} \coloneqq (e_{\text{arc}}, e_2, \ldots, e_r) \in (-L/2, L/2] \times \mathbb{R}^{r-1}$.

Remark 4.2.2. When $\theta(t) = t$ the definition of the errors (4.4) simplifies to

$$\begin{aligned} e_1(t) &= \eta_1(t) - \operatorname{mod}(Qw(t), L) \\ e_i(t) &= \eta_i(t) - QS^{i-1}w(t), \qquad i \in \{2, \ldots, r\}. \end{aligned}$$

◀

The structure of the η-dynamics in the path following normal form (3.19) gives

$$\begin{aligned}
\dot{e}_{\text{arc}} &= e_2 \\
\dot{e}_2 &= e_3 \\
&\cdots \\
\dot{e}_r &= L^r_{A_p x} h_{\text{PF},1}(x) + L_{B_p} L^{r-1}_{A_p x} h_{\text{PF},1}(x) u_p - \frac{\mathrm{d}^r}{\mathrm{d}t^r} Q w(\theta(t)).
\end{aligned}$$

Theorem 4.2.3. *Consider a minimum phase L.T.I. system (4.1) assigned a curve in its output space satisfying all the assumptions of Section 3.1 and a desired motion along the curve generated by the exosystem (4.2). Consider the full information feedback control law*

$$u_p = \left(C_p A_p^{r-1} B_p\right)^{-1} \left(\frac{\partial F_{\text{PF}}}{\partial y}\bigg|_{y=C_p x} \right)^{-1} \left(-L^r_{A_p x} h_{\text{PF}}(x) + \begin{bmatrix} v^{\parallel} \\ v^{\pitchfork} \end{bmatrix} \right) \tag{4.5}$$

with

$$\begin{aligned}
v^{\parallel} &= K_\eta \mathbf{e} + \frac{\mathrm{d}^r}{\mathrm{d}t^r} Q w(\theta) = -k_{\eta,1} e_{\text{arc}} - k_{\eta,2} e_2 - k_{\eta,3} e_3 - \cdots - k_{\eta,r} e_r + \frac{\mathrm{d}^r}{\mathrm{d}t^r} Q w(\theta) \\
v^{\pitchfork} &= \mathbf{K}_\xi \xi = \begin{bmatrix} K_{\xi,2} \xi^2 \\ K_{\xi,3} \xi^3 \\ \cdots \\ K_{\xi,m} \xi^m \end{bmatrix}
\end{aligned} \tag{4.6}$$

where K_η and $\mathbf{K}_\xi$ are selected so that, respectively, $A + bK_\eta$ and $\mathbf{A} + \mathbf{B}\mathbf{K}_\xi$ are Hurwitz. Then there exists an open set containing $\Gamma_\star$ such that the closed-loop system satisfies the three objectvies of the path following problem.

Proof. By Proposition 3.4.1, system (4.1) is differentially equivalent to a system with the

path following normal form (3.19) in an open set containing (3.18). Using Corollary 3.3.1 the feedback (4.5) is well-defined in a neighbourhood of $\Gamma_\star$ and therefore the system (4.1) is feedback equivalent to the system

$$\begin{aligned}\dot{\zeta} &= A_{00}\zeta + A_{01}F_{\mathrm{PF}}^{-1}(y_{\mathrm{PF}})\\ \dot{\eta} &= A\eta + bv^{\parallel}\\ \dot{\xi} &= \mathbf{A}\xi + \mathbf{B}v^{\pitchfork}\end{aligned}$$

in a neighbourhood of $\Gamma_\star$. Transform the tangential dynamics (η-dynamics) into the tangential tracking errors to get

$$\begin{aligned}\dot{\zeta} &= A_{00}\zeta + A_{01}F_{\mathrm{PF}}^{-1}(y_{\mathrm{PF}})\\ \dot{\mathbf{e}} &= A\mathbf{e} + b\left(v^{\parallel} - \frac{\mathrm{d}^r}{\mathrm{d}t^r}Qw(\theta(t))\right)\\ \dot{\xi} &= \mathbf{A}\xi + \mathbf{B}v^{\pitchfork}.\end{aligned}$$

If we substitute the expressions (4.6) for the auxiliary controls we get the closed-loop dynamics

$$\begin{aligned}\dot{\zeta} &= A_{00}\zeta + A_{01}F_{\mathrm{PF}}^{-1}(y_{\mathrm{PF}})\\ \dot{\mathbf{e}} &= (A + bK_\eta)\mathbf{e}\\ \dot{\xi} &= (\mathbf{A} + \mathbf{B}\mathbf{K}_\xi)\xi.\end{aligned}$$

Since $\xi = 0$ is an equilibrium of the ξ-subsystem we get invariance of $\{x : \xi = 0\} \subset \Gamma_\star$. Furthermore, by the construction of the gains K_η and $\mathbf{K}_\xi$ we get that $\xi = 0$ and $\mathbf{e} = 0$ are locally exponentially stable. Finally, since the system is minimum phase, A_{00} is Hurwitz. Therefore, since the curve $\mathcal{C}$ is bounded, $F_{\mathrm{PF}}(y_{\mathrm{PF}})$ is bounded and hence ζ and u_p are bounded. □

Remark 4.2.4. The invariant subset $\{x \in \mathbb{R}^n : \xi = 0\} \subset \Gamma_\star$ contains all those motions of the control system whose associated output signal lies on the assigned curve $\mathcal{C}$. It is a proper subset of $\Gamma_\star$ because the output does not need to be constant. It just needs to be on the path. Thus, if $\xi(0) = 0$ but $e_{\text{arc}}(0) \neq 0$, the closed-loop system will track the desired motion generated by the exosystem but it will not leave the path.

Chapter 5

Synchronized Path Following

Consider a homogenous multi-agent system with $N \in \mathbb{N}$ agents modelled by identical linear, time-invariant, square plants with no feed through of the form:

$$\dot{x}_i(t) = A_p x_i(t) + B u_{p,i}(t), \qquad i \in \mathbb{N}_N, \tag{5.1a}$$

$$y_i(t) = C_p x_i(t). \tag{5.1b}$$

We assume throughout that the pair (A_p, B_p) is controllable, the triple (C_p, A_p, B_p) has vector relative degree $\{r, \ldots, r\}$ and that the systems are minimum phase.

Each agent is assigned a (possibly distinct) closed curve in its output space and is tasked with following its assigned curve while synchronizing its postion along the path with the other agents in the system. The agents exchange information with each other in order to synchronize.

5.1 Inter-Agent Communication

Communication between systems is modelled by an undirected graph $\mathcal{G} = (\mathcal{V}, \mathcal{E})$ with vertex set $\mathcal{V} = \{v_1, \ldots, v_N\}$, arc set $\mathcal{E} \subset \mathcal{V} \times \mathcal{V}$, and adjacency matrix $A_{\mathcal{G}}$. The vertex $v_k \in \mathcal{V}$ represents the kth system. The (j,k)th entry of the adjacency matrix $A_{\mathcal{G}}$, denoted a_{jk}, equals the number of edges from vertex j to vertex k. This means $\{v_j, v_k\} \in \mathcal{E}$ if, and only if, $a_{kj} \neq 0$ and indicates that systems j and k can exchange information.

The Laplacian matrix $L_{\mathcal{G}}$ associated to the graph $\mathcal{G}$ is defined element-wise to be

$$[L_{\mathcal{G}}]_{kj} \coloneqq \begin{cases} \sum_{i=1}^{N} a_{ki}, j = k \\ -a_{kj}, j \neq k. \end{cases}$$

Definition 5.1.1. An undirected graph $\mathcal{G}$ is **connected** if for any two distinct vertices $v_i, v_j \in \mathcal{V}$, there is a sequence of edges in $\mathcal{E}$ connecting v_i and v_j. ♦

We make the following assumption throughout this chapter.

Assumption 4 (Connected communication graph)**.** *The undirected graph $\mathcal{G}$ modelling information flow in the multi-agent system is connected.* ◀

In practice, the curves that each agent must follow may be spatially far apart eroding the ability to communicate and making the communication graph time-varying. Assumption 4 idealizes the way that agents communicate. Furthermore, there are no constraints in terms of channel capacity though as we will see, the proposed solution does not require large amounts of data exchange.

5.2 Synchronization

Agent i is assigned a closed-curve $\mathcal{C}_i$ which satisfies all of the assumptions from Section 3.1. We do not assume that $\mathcal{C}_i$ equals $\mathcal{C}_j$ and therefore the paths in general have different lengths L_i and L_j. The desired motion along each path is generated by an exosystem which, for the purposes of synchronization, is slightly different than the one considered in Assumption 2.

Assumption 5 (Common Exosystem Dynamics)**.** *The desired motion for agent $i \in \mathbb{N}_N$ along its assigned curve $\mathcal{C}_i$ is generated as the output of a system of the form*

$$\begin{aligned} \frac{\mathrm{d}}{\mathrm{d}t} w_i(\theta(t)) &= \frac{\mathrm{d}\theta}{\mathrm{d}t} S w_i(\theta(t)), \qquad w_i(\theta(0)) = w_{i,0} \\ r_i(\theta(t)) &= \sigma_i \left(\frac{L_i}{2\pi} \bmod (Q w_i(\theta(t)), 2\pi) \right) \end{aligned} \tag{5.2}$$

where $\sigma(S) \subset \mathbb{C}^- \cup j\mathbb{R}$, $Q \in \mathbb{R}^{1 \times \dim(w_i)}$ and $\theta(t) = ct + t_0$ where $c > 0$ and t_0 are constants.

Under Assumption 5, every agent's exosystem uses the same matrices S and Q as well as the same timing law θ. Different motions result from (i) different initial conditions $w_{i,0}$ and (ii) different curve parameterizations σ_i. The fact that each agent uses the same S, Q, and θ is motivated by [41, Theorem 3] which roughly states that a necessary condition for output synchronization is that all the agents use a copy of the *same* exosystem.

By Proposition 4.1.1, having the system output track the desired motion generated by (5.2) is equivalent to having $s_i(y_i) = 0$ so that agent i is on its path and $\varpi_i(y_i) = \frac{L_i}{2\pi} \bmod (Q w_i(\theta(t)), 2\pi)$. With this in mind, we now give an interpretation of what it means to be synchronized.

Definition 5.2.1. The **synchronization error** between agents $i, j \in \mathbb{N}_N$ is given by

$$e_{\text{sync}}^{(i,j)} \coloneqq \frac{1}{2\pi}\text{dist}_{\mathbb{S}}\left(\exp\left(j\frac{2\pi}{L_i}\eta_{i,1}\right), \exp\left(j\frac{2\pi}{L_j}\eta_{j,1}\right)\right). \tag{5.3}$$

The agents are said to be performing **synchronized path following** at time t if $y_i(t) \in \mathcal{C}_i$, $y_j(t) \in \mathcal{C}_j$ and $e_{\text{sync}}^{(i,j)}(t) = 0$. ♦

The synchronization error is defined by first normalizing each agent's position on the path $\eta_{i,1}$ to a percentage of a revolution around the path. Next, the difference is multiplied by 2π so that the complex exponential generates a point on the circle. We compute the signed distance between the points on the circle and finally normalize the synchronization error to between $(-0.5, 0.5]$ so that it can be interpreted in terms of revolutions of the path.

The synchronized path following problem considered here is to drive $e_{\text{synch}}^{(i,j)}$ to zero for all $i, j \in \mathbb{N}_N$ while simultaneously driving the agents to their paths $y_i \to \mathcal{C}_i$ as $t \to \infty$. We would like each agent's controller to render its assigned path controlled invariant.

Proposition 5.2.2. *Let $i, j \in \mathbb{N}_N$. If there exists a time t at which $w_i(t) = w_j(t)$ and*

$$\eta_{i,1}(t) = \frac{L_i}{2\pi} \bmod (Qw_i(\theta(t)), 2\pi), \qquad \eta_{j,1}(t) = \frac{L_j}{2\pi} \bmod (Qw_j(\theta(t)), 2\pi),$$

then $e_{\text{synch}}^{(i,j)}(t) = 0$.

Proof. Using the definition (5.3) of synchronization error we have

$$\begin{aligned} e_{\text{synch}}^{(i,j)}(t) &= \frac{1}{2\pi}\text{dist}_{\mathbb{S}}\left(\exp\left(j\frac{2\pi}{L_i}\eta_{i,1}\right), \exp\left(j\frac{2\pi}{L_j}\eta_{j,1}\right)\right) \\ &= \frac{1}{2\pi}\text{dist}_{\mathbb{S}}\left(\exp\left(j \bmod (Qw_i(\theta(t)), 2\pi)\right), \exp\left(j \bmod (Qw_j(\theta(t)), 2\pi)\right)\right). \end{aligned}$$

Since $w_i(t) = w_j(t)$ the claim follows immediately. □

In principle then, one way to solve the synchronized path following problem posed here is to have all the agents agree on a common initial condition for their exosystems and then have each of the agents employ the controllers proposed in Chapter 4. A more robust solution is to leverage the results in [37] and [41] and have each agent modify its local copy of the exosystem using the information available from its neighbours.

Theorem 5.2.3 (Convergence of Exosystems)**.** *Consider N systems of the form*

$$\frac{\mathrm{d}}{\mathrm{d}t} w_i(\theta(t)) = cSw_i(\theta(t)) + v_i(t), \qquad w_i(\theta(0)) = w_{i,0}, \tag{5.4}$$

where $\sigma(S) \subset \mathbb{C}^- \cup j\mathbb{R}$, $c > 0$ and $v_i(t)$ is a control input. If

$$v_i(t) = \sum_{j=1}^{N} a_{ij}(w_j(\theta(t)) - w_i(\theta(t))) \tag{5.5}$$

where a_{ij} is the (i,j)th entry of the adjacency matrix $A_{\mathcal{G}}$ associated with a connected communication graph $\mathcal{G}$, then there is a solution of $\dot{w}_0 = Sw_0$ to which $w_i(t)$, for all $i \in \mathbb{N}_N$, exponentially converges.

More formally, Theorem 5.2.3 says that

$$(\forall i \in \mathbb{N}_N)(\forall t \geq 0)(\exists \delta, \lambda > 0)(\exists w_0(0) \in \mathbb{R}^{\dim(w_i)}) \|w_i(t) - \mathrm{e}^{cSt} w_0(0)\| \leq \delta \mathrm{e}^{-\bar{\lambda} t} \|w_i(0) - w_0(0)\|.$$

Proof. Consider the exosystem dynamics (5.4) with feedback control input (5.5) and apply the time-varying coordinate change

$$q_i(t) = \mathrm{e}^{-cSt} w_i(\theta(t)), \qquad i \in \mathbb{N}_N.$$

Then

$$\begin{aligned}\dot{q}_i &= -cS\mathrm{e}^{-cSt}w_i(\theta(t)) + c\mathrm{e}^{-cSt}Sw_i(\theta(t)) + \mathrm{e}^{-cSt}\sum_{j=1}^{N} a_{ij}(w_j - w_i) \\ &= \mathrm{e}^{-cSt}\sum_{j=1}^{N} a_{ij}(w_j - w_i) \\ &= \sum_{j=1}^{N} a_{ij}(q_j - q_i).\end{aligned}$$

Stacking this differential equation for each $i \in \mathbb{N}_N$ into a vector we obtain

$$\dot{q} = -(L_{\mathcal{G}} \otimes I_{\dim(w_i)})q$$

where $\otimes$ is the Kronecker product. By assumption $\mathcal{G}$ is connected. Therefore, using well-known results on consensus algorithms [19, Proposition 5.3], all the $q_i(t)$ exponentially converge to a common constant $w_0 \in \mathbb{R}^{\dim(w_i)}$ as $t \to \infty$. This means that there exists $\delta, \lambda > 0$ such that

$$(\forall i \in \mathbb{N}_N) \;\; \|q_i(t) - w_0\| \leq \delta \mathrm{e}^{-\lambda t}\|q_i(0) - w_0\|.$$

Using the fact that $q_i(t) = \mathrm{e}^{-cSt}w_i(\theta(t))$ we have that

$$\begin{aligned}&\|\mathrm{e}^{-cSt}w_i(\theta(t)) - w_0\| \leq \delta \mathrm{e}^{-\lambda t}\|w_i(\theta(0)) - w_0\| \\ \Rightarrow\; &\|\mathrm{e}^{-cSt}\left(w_i(\theta(t)) - \mathrm{e}^{cSt}w_0\right)\| \leq \delta \mathrm{e}^{-\lambda t}\|w_i(\theta(0)) - w_0\| \\ \Rightarrow\; &\|\mathrm{e}^{cSt}\|\|\mathrm{e}^{-cSt}\left(w_i(\theta(t)) - \mathrm{e}^{cSt}w_0\right)\| \leq \delta \mathrm{e}^{-\lambda t}\|\mathrm{e}^{cSt}\|\|w_i(\theta(0)) - w_0\|.\end{aligned}$$

Using the triangle inequality we have

$$\|\mathrm{e}^{cSt}\mathrm{e}^{-cSt}\left(w_i(\theta_i(t)) - \mathrm{e}^{cSt}w_0\right)\| \leq \|\mathrm{e}^{cSt}\|\|\mathrm{e}^{-cSt}\left(w_i(\theta(t)) - \mathrm{e}^{cSt}w_0\right)\|.$$

Combining these inequalities yields

$$\Rightarrow \ \|w_i(t) - \mathrm{e}^{cSt}w_o\| \leq \delta\mathrm{e}^{-\lambda t}\|\mathrm{e}^{cSt}\|\|w_i(\theta(0)) - w_o\|.$$

As all the eigenvalues of the matrix cS have at most zero real part, there exists a constant $\bar{\lambda} > 0$ such that

$$\Rightarrow \ \|w_i(t) - \mathrm{e}^{cSt}w_o\| \leq \delta\mathrm{e}^{-\bar{\lambda}t}\|w_i(\theta(0)) - w_o\|.$$

□

Remark 5.2.4. As noted in [37, Remark 1], If S were to have eigenvalues with a positive real part, it is important that $\mathcal{G}$ satisfy Assumption 4 in order for the exponential synchronization of (5.4) to dominate over the instability of S.

Theorem 5.2.3, in conjunction with the controllers from Theorem 4.2.3, suggest a viable solution to the synchronized path following problem. Each agent uses the consensus algorithm of Theorem 5.2.3 to modify its local copy of the exosystem. At the same time, the individual systems employ a feedback controller of the form found in Theorem 4.2.3. What results is that each agent approaches its assigned path, each agent tracks the reference trajectory generated by its exosystem and simultaneously, all the exosystems converge to a common trajectory. We formalize this result because there is some subtly in the stability analysis.

Define, for each agent $i \in \mathbb{N}_N$, the errors

$$\begin{aligned} e_{i,1}(t) &= \eta_{i,1}(t) - \operatorname{mod}(Qw_i(t), L_i) \\ e_{i,j}(t) &= \eta_{i,j}(t) - c^{j-1}QS^{j-1}w_i(\theta(t)), \qquad j \in \{2, \dots, r\}. \end{aligned} \tag{5.6}$$

Further define $e_{i,\text{arc}}$ as per Definition 4.2.1. As in Chapter 4, the chain rule gives that $\dot{e}_{i,\text{arc}} = \dot{e}_{i,1}$. Note however that if we are using the consensus algorithm from Theorem 5.2.3, then it is *no longer true* that $\dot{e}_{i,j} = e_{i,j+1}$ for $j \in \{1, \dots, r-1\}$. Instead we get, again using the structure of the η-dynamics in the path following normal form (3.19), the differential equations

$$\begin{aligned} \dot{e}_{i,\text{arc}} &= e_{i,2} - Qv_i \\ \dot{e}_{i,2} &= e_{i,3} - cQSv_i \\ &\dots \\ \dot{e}_{i,r-1} &= e_{i,r} - c^{r-2}QS^{r-2}v_i \\ \dot{e}_{i,r} &= L^r_{A_p x_i} h_{\text{PF}_i,1}(x_i) + L_{B_p} L^{r-1}_{A_p x_i} h_{\text{PF}_i,1}(x_i) u_{p,i} - c^r QS^r w_i - c^{r-1}QS^{r-1}v_i \end{aligned}$$

where $v_i = \sum_{j=1}^N a_{ij}(w_j(\theta(t)) - w_i(\theta(t)))$. Define $\mathbf{e}^{(i)} \coloneqq (e_{i,\text{arc}}, e_{i,2}, \dots, e_{i,r})$. We are now ready to state the main result of this Chapter.

Theorem 5.2.5. *Consider the multi-agent system (5.1) with a connected communication graph where each agent is assigned a curve in its output space satisfying all the assumptions of Section 3.1. Each system is given a desired motion along the curve generated by the exosystem (5.2). Suppose that each agent modifies its exosystem according to (5.4) and (5.5)*

and selects the feedback control law

$$u_{p,i} = \left(C_p A_p^{r-1} B_p\right)^{-1} \left(\frac{\partial F_{\mathrm{PF}_i}}{\partial y}\bigg|_{y_i = C_p x_i} \right)^{-1} \left(-L^r_{A_p x_i} h_{\mathrm{PF}_i}(x_i) + \begin{bmatrix} v^{i,\parallel} \\ v^{i,\pitchfork} \end{bmatrix} \right) \tag{5.7}$$

with

$$\begin{aligned} v^{i,\parallel} &= K_\eta^{(i)} \mathbf{e}^{(i)} + c^r Q S^r w_i \\ v^{i,\pitchfork} &= \mathbf{K}_\xi^{(i)} \xi^{(i)} \end{aligned} \tag{5.8}$$

where $K_\eta^{(i)}$ and $\mathbf{K}_\xi^{(i)}$ are selected so that, respectively, $A + bK_\eta^{(i)}$ and $\mathbf{A} + \mathbf{B}\mathbf{K}_\xi^{(i)}$ are Hurwitz. Then there exists an open set of initial conditions where the three objectvies of the synchronized path following problem are achieved.

Proof. Following the same argument as in the proof of Theorem 4.2.3, using the proposed controllers, each agent is feedback equivalent to the system

$$\begin{aligned} \dot{w}_i &= cSw_i(\theta) + \sum_{j=1}^N a_{ij}(w_j(\theta) - w_i(\theta)) \\ \dot{\zeta}^{(i)} &= A_{00}\zeta^{(i)} + A_{01} F^{-1}_{\mathrm{PF}_i}(y_{\mathrm{PF}_i}) \\ \dot{\mathbf{e}}^{(i)} &= (A + bK_\eta^{(i)})\mathbf{e}^{(i)} + \begin{bmatrix} Q \\ cQS \\ \cdots \\ c^{r-1}QS^{r-1} \end{bmatrix} \sum_{j=1}^N a_{ij}(w_j(\theta) - w_i(\theta)) \\ \dot{\xi}^{(i)} &= (\mathbf{A} + \mathbf{B}\mathbf{K}_\xi^{(i)})\xi^{(i)}. \end{aligned}$$

Since $\xi^{(i)} = 0$ is an equilibrium of the $\xi^{(i)}$-subsystem we get invariance of $\left\{x_i : \xi^{(i)} = 0\right\}$. By definition of the ξ-states, points on this invariant set result in the output of the system being on its path $\mathcal{C}_i$. By the construction of the gain $\mathbf{K}_\xi^{(i)}$ we get that $\xi^{(i)} = 0$ is locally

exponentially stable. This shows that agent i approaches its path $\mathcal{C}_i$.

By Theorem 5.2.3, the consensus error between exosystems converges to zero exponentially so that the sum $\sum_{j=1}^{N} a_{ij}(w_j(\theta) - w_i(\theta))$ goes to zero exponentially. By the construction of the gains $K_\eta^{(i)}$, $A + bK_\eta^{(i)}$ is Hurwitz. Therefore we have an exponentially stable linear system being driven by a forcing function that is decaying to zero exponentially fast. This allows us to conclude that $\mathbf{e}^{(i)} = 0$ is locally exponentially stable. By Proposition 5.2.2 this implies that $e_{\text{synch}}^{(i,j)}$ approaches zero for all $i, j \in \mathbb{N}_N$.

Finally, since each system is minimum phase A_{00} is Hurwitz. Therefore, since the curve $\mathcal{C}_i$ is bounded, $F_{\text{PF}}(y_{\text{PF}_i})$ is bounded and hence $\zeta^{(i)}$ and $u_{p,i}$ are bounded. □

Chapter 6

Laboratory Results

In this chapter we illustrate the effectiveness of the controllers from Chapters 4 and 5 through simulation and through implementation on mobile robots following circular paths.

6.1 Differential Drive Robot Model

We consider a multi-agent system consisting of two differential drive robots whose kinematic models are given by

$$\begin{aligned} \begin{bmatrix} \dot{x}_{i,1} \\ \dot{x}_{i,2} \\ \dot{x}_{i,3} \end{bmatrix} &= \begin{bmatrix} u_{i,1}\cos(x_{i,3}) \\ u_{i,1}\sin(x_{i,3}) \\ u_{i,2} \end{bmatrix} \\ \begin{bmatrix} y_{i,1} \\ y_{i,2} \end{bmatrix} &= \begin{bmatrix} x_{i,1} + \ell\cos(x_{i,3}) \\ x_{i,2} + \ell\sin(x_{i,3}) \end{bmatrix}, \qquad \ell \in \mathbb{R} \setminus \{0\} \end{aligned} \tag{6.1}$$

where $i \in \mathbb{N}_2$. For each system, $x_i \in \mathbb{R}^2 \times \mathbb{S}$ is the state vector, $u_i := \text{col}(u_{i,1}, u_{i,2}) \in \mathbb{R}^2$ where $u_{i,1}$ and $u_{i,2}$ are the linear and angular velocity inputs, respectively, and $y_i \in \mathbb{R}^2$ is the output. The first two plant states correspond to the (x_1, x_2)-planar position of the robot's centre of mass with the third state being its heading angle with respect to the positive x_1-axis (see Figure 6.1 below).

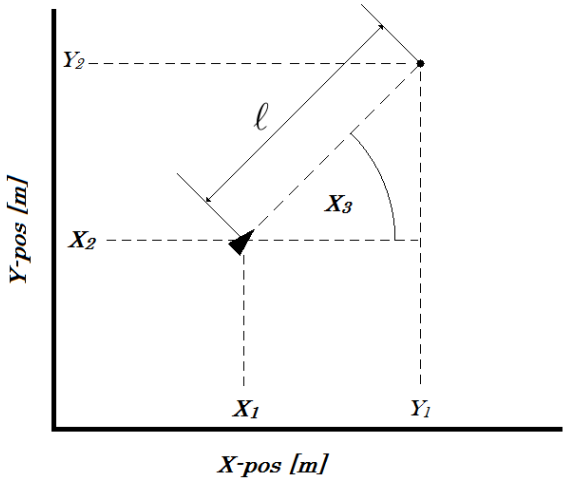

Figure 6.1: Schematic Diagram of a differential drive robot.

The output is taken to be a point $\ell \neq 0$ units from the robot along its directional heading as illustrated in Figure 6.1, in order to avoid singularities.

Lemma 6.1.1. *System 6.1 has relative degree* $\{1, 1\}$

Proof. For now, drop the subscript i in the plant model and note that this is a plant of the form (2.3) with $m = 2$ and

$$f(x) = 0, \qquad g_1(x) = \begin{bmatrix} \cos(x_3) \\ \sin(x_3) \\ 0 \end{bmatrix}, \qquad g_2(x) = \begin{bmatrix} 0 \\ 0 \\ 1 \end{bmatrix}$$

and

$$h_1(x) = x_1 + \ell\cos(x_3), \qquad h_2(x) = x_2 + \ell\sin(x_3).$$

To prove the lemma the conditions of Definition 2.4.1 are checked. The first condition is trivially satisfied as there are no elements in the set. For the second condition, calculating the entries in the decoupling matrix gives

$$\begin{aligned}\det\left(\begin{bmatrix} L_{g_1}h_1(x) & L_{g_2}h_1(x) \\ L_{g_1}h_2(x) & L_{g_2}h_2(x) \end{bmatrix}\right) &= \det\left(\begin{bmatrix} \cos(x_3) & -\ell\sin(x_3) \\ \sin(x_3) & \ell\cos(x_3) \end{bmatrix}\right) \\ &= \ell\cos^2(x_3) + \ell\sin^2(x_3) \\ &= \ell.\end{aligned}$$

As $\ell \neq 0$ by assumption, all the conditions of Definition 2.4.1 have been satisfied with $\{r, r\} = \{1, 1\}$. □

Remark 6.1.2. The model used here is idealized and very simplistic. Some phenomena the model does not take into account are traction availability and motor responses (i.e., dynamics). The concrete floor of the testing ground is dusty and a low coefficient of friction is observed between it and the wheels of the robot. When a command signal is too high this low coefficient of friction causes the wheel to spin in place and slippage occurs. Any rotating mass induces a moment of inertia which is a measure of how resistant the mass is to changes in its angular velocity. A typical DC motor has a first order step response for voltage input to angular velocity output. The model ignores this and assumes any commanded angular velocity is applied immediately. ◀

We put each system into its Byrnes-Isidori normal form by defining the coordinate

transformation (again dropping the subscript i)

$$T : \mathbb{R}^2 \times \mathbb{S} \to \mathbb{R}^2 \times \mathbb{S}$$
$$x \mapsto \begin{bmatrix} x_1 + \ell \cos(x_3) \\ x_2 + \ell \sin(x_3) \\ x_3 \end{bmatrix}.$$

If we let $(q_1, q_2, z) = T(x)$ then the inverse of the function is given by

$$T^{-1}(q, z) = \begin{bmatrix} q_1 - \ell \cos(z) \\ q_2 - \ell \sin(z) \\ z \end{bmatrix}$$

from which we see that T is a global diffeomorphism. As a result, selecting the preliminary feedback

$$u = \frac{1}{\ell} \begin{bmatrix} \ell \cos(x_3) & \ell \sin(x_3) \\ -\sin(x_3) & \cos(x_3) \end{bmatrix} \begin{bmatrix} v_1 \\ v_2 \end{bmatrix}$$

causes the unicycle models (6.1) to be globally feedback equivalent to

$$\begin{aligned} \dot{z} &= \frac{1}{\ell}(-\sin(z)v_1 + \cos(z)v_2) \\ \dot{q}_1 &= v_1 \\ \dot{q}_2 &= v_2 \\ y &= \begin{bmatrix} q_1 \\ q_2 \end{bmatrix}. \end{aligned} \tag{6.2}$$

Although system (6.2) is not L.T.I., we will use it to illustrate the results of this thesis

by essentially ignoring the nonlinear z_i-dynamics. In this case, since $z_i = x_{i,3} \in \mathbb{S}$, the state is always bounded so there is some justification in doing so. Thus we have taken

$$A_p = 0, \qquad B_p = I_2, \qquad C_p = I_2.$$

6.1.1 Circular Paths

In order to conduct experiments with the simplest possible implementation, the simplest type of closed curve is used, a circle. All circles are centered at the origin with varying radii. Each circle produces a curve for the output y_i to track with smooth parameterization

$$\begin{aligned} \sigma_i : \mathbb{T}_i &\to \mathbb{R}^2 \\ \lambda_i &\mapsto R_i \begin{bmatrix} \cos(\lambda_i / R_i) \\ \sin(\lambda_i / R_i) \end{bmatrix} \end{aligned}$$

where R_i is the radius of the circle to follow. The arc-length of path i is $L_i = 2\pi R_i$. This curve satisfies all the criteria of Section 3.1. In particular, Assumption 1 is satisfied with

$$s_i(y_i) = y_{i,1}^2 + y_{i,2}^2 - R_i^2.$$

To avoid collisions in the M.A.S. case, care is taken to avoid initial conditions that would lead to collision trajectories. The difference in radii is also kept greater than two-and-a-half times that of the diameter of the robot as it sits upright.

6.2 Implementation

Multiple two-wheeled, differential drive, autonomous TURTLEBOT2 robots from Clearpath Robotics are used for physical experiments. The robots are controlled through the R.O.S. on a laptop running in a linux environment via a Ubuntu operating system. A R.O.S. version is called a distribution and it is the collection of officially released R.O.S. packages all belonging to the same version number. The R.O.S. distribution used is ROS INDIGO IGLOO with Ubuntu version 14.04, nicknamed Trusty Tahr.

Figure 6.2: Turtlebot II robot from Clearpath Robotics

Each laptop is connected to a common router wirelessly and can interact with a VICON motion capture camera system to obtain positional information. The interaction is aided by the use of R.O.S. package VRPN_CLIENT_ROS. The VICON motion capture system has a total of sixteen (16) cameras whose field of view overlap to cover the entire testing grounds in which the experiment takes place. The testing area is a concrete floor with dimensions 4.5×4.5 $[m^2]$ located indoors. This also helps avoid unnecessary disturbances such as wind and rain from entering the experiments.

Communication between laptops is made possible with the R.O.S. package MULTIMASTER_FKIE. Technical report [21] is used to configure the laptops so that two or more R.O.S. networks act as one. To showcase the distributed nature of the solution only the normalized reference signals are passed between robots which then carry out all necessary computations using only on-board processors.

6.3 Path Following Normal Form

The simple nature of the curves simplifies the expression of the projection (3.4). This gives a very simple form for the path following output (3.6)

$$\begin{aligned} F_{\mathrm{PF}} : \mathbb{R}^2 \backslash \{0\} &\to \mathbb{T} \times \mathbb{R} \\ y &\mapsto \begin{bmatrix} R_i \mathrm{atan2}\left(\frac{y_{i,2}}{y_{i,1}}\right) \\ y_{i,1}^2 + y_{i,2}^2 - R_i^2 \end{bmatrix} \end{aligned} \tag{6.3}$$

where atan2 is a branch of the 4-quadrant arctangent function with codomain $(-\pi, \pi]$.

To put the system into the path following normal form, we use the coordinate change (3.7) with

$$\begin{aligned} \zeta_i &= z_i \\ \eta_{i,1} &= R_i \mathrm{atan2}\left(\frac{q_{i,2}}{q_{i,1}}\right) \\ \xi_{1,i}^2 &= q_{i,1}^2 + q_{i,2}^2 - R_i^2. \end{aligned}$$

Then the path following normal form is given by

$$\begin{aligned} \dot{\zeta}_i &= \frac{1}{\ell}\left(-\sin\left(\zeta_i\right) v_{i,1} + \cos\left(\zeta_i\right) v_{i,2}\right) \\ \dot{\eta}_{i,1} &= \frac{R_i}{q_{i,1}^2 + q_{i,2}^2}\left(-q_{i,2} v_{i,1} + q_{i,1} v_{i,2}\right) \\ \dot{\xi}_{1,i}^2 &= 2 q_{i,1} v_{i,1} + 2 q_{i,2} v_{i,2}. \end{aligned}$$

The feedback (4.5) simplifies to

$$\begin{aligned}\begin{bmatrix} v_{i,1} \\ v_{i,2} \end{bmatrix} &= (C_p B_p)^{-1} \left(\frac{\partial F_{\mathrm{PF}_i}}{\partial y_i} \right)^{-1} \begin{bmatrix} v^{i,\parallel} \\ v^{i,\pitchfork} \end{bmatrix} \\ &= \begin{bmatrix} \frac{-R_i q_{i,2}}{q_{i,1}^2 + q_{i,2}^2} & \frac{R_i q_{i,1}}{q_{i,1}^2 + q_{i,2}^2} \\ 2q_{i,1} & 2q_{i,2} \end{bmatrix}^{-1} \begin{bmatrix} v^{i,\parallel} \\ v^{i,\pitchfork} \end{bmatrix}.\end{aligned}$$

This feedback is well-defined on $\mathbb{R}^2 \setminus \{0\}$ and so the unicycles are almost globally feedback equivalent to

$$\begin{aligned}\dot{\zeta}_i &= \frac{1}{\ell} \left(\frac{1}{R_i} \left(q_{i,1} \cos(\zeta_i) + q_{i,2} \sin(\zeta_i) \right) v^{i,\parallel} + \frac{R_i}{2(q_{i,1}^2 + q_{i,2}^2)} \left(q_{i,2} \cos(\zeta_i) - q_{i,1} \sin(\zeta_i) \right) v^{i,\pitchfork} \right) \\ \dot{\eta}_{i,1} &= v^{i,\parallel} \\ \dot{\xi}_{1,i}^2 &= v^{i,\pitchfork} \\ y_{\mathrm{PF}_i} &= \begin{bmatrix} \eta_{i,1} \\ \xi_{1,i}^2 \end{bmatrix}.\end{aligned} \tag{6.4}$$

6.4 Path Following with a Single Robot

In this section, we present laboratory results for a single agent so we drop the i notation. As always, the goal is for a single agent to reach a curve in its output space such that the curve is made invariant. A ramp function is chosen as the reference (4.2) for η with timing

law $\theta(t) = t$ so that

$$S = \begin{bmatrix} 0 & 1 \\ 0 & 0 \end{bmatrix}, \qquad Q = \begin{bmatrix} 1 & 0 \end{bmatrix}.$$

This produces a saw-tooth waveform in $\mathbb{T}$ meaning that the robot should continuously loop around its path. In this case the tangential and transversal controllers (4.6) simplify to

$$v^{\parallel} = k_\eta e_{\text{arc}} + QSw = k_\eta R \text{dist}_{\mathbb{S}} \left(\exp\left(j\frac{\eta}{R}\right), \exp\left(j\frac{1}{R} \bmod (w_1(t), 2\pi R)\right)\right) + w_2(t)$$

$$v^{\pitchfork} = k_\xi \xi$$

with k_η, $k_\xi < 0$. Notice that each subsystem of the path following normal form is one dimensional so the gains are scalars.

Two test cases are shown to illustrate that the purposed control law (4.5) works in practice. The differences between cases are highlighted in Table 6.1 with parameter values listed in Table 6.2. Stability of $\xi = 0$ can be seen in Figures 6.5 and 6.9 for each test case respectively. The fact that the tangential state tracks the ramp signal is shown in Figures 6.6 and 6.10 for each test case respectively. This is also shown in the arc-error plots witch are plots of e_{arc} versus time.

Test Case	R [m]	$x_1(0)$ [m]	$x_2(0)$ [m]	$x_3(0)$ [rad]	$w_1(0)$	$w_2(0)$
1	1	1.96	0.97	3.04	0	0.3
2	2	0.84	0.12	1.08	0	0.4

Table 6.1: Single Agent Initial Conditions

Parameter	Value
K_ξ	-20
K_η	-10
$\theta(t)$	t
ℓ	0.2 [m]

Table 6.2: Single Agent Parameter Values

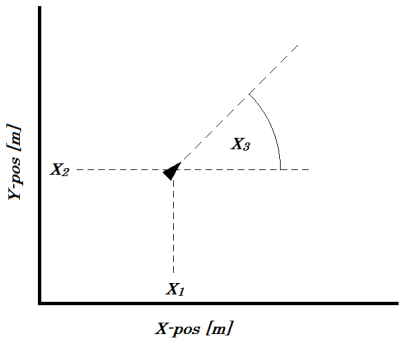

Figure 6.3: Orientation Marker

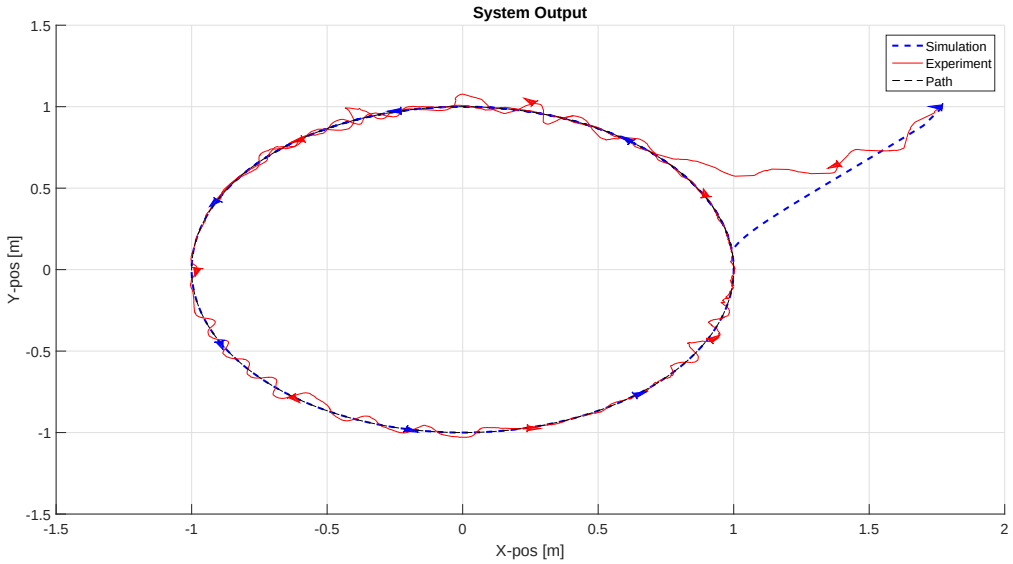

Figure 6.4: System Output - Test Case 1

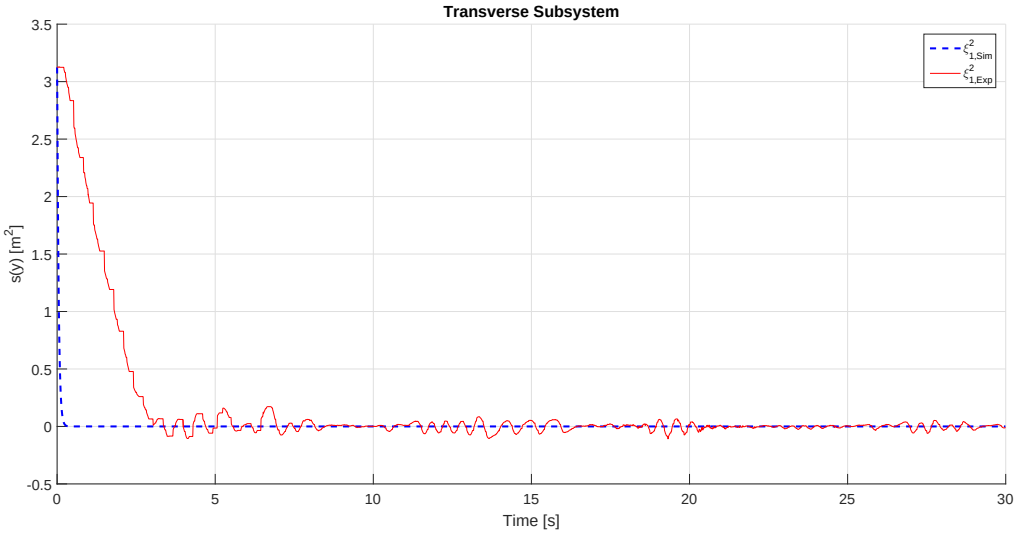

Figure 6.5: Transverse Subsystem (ξ) - Test Case 1

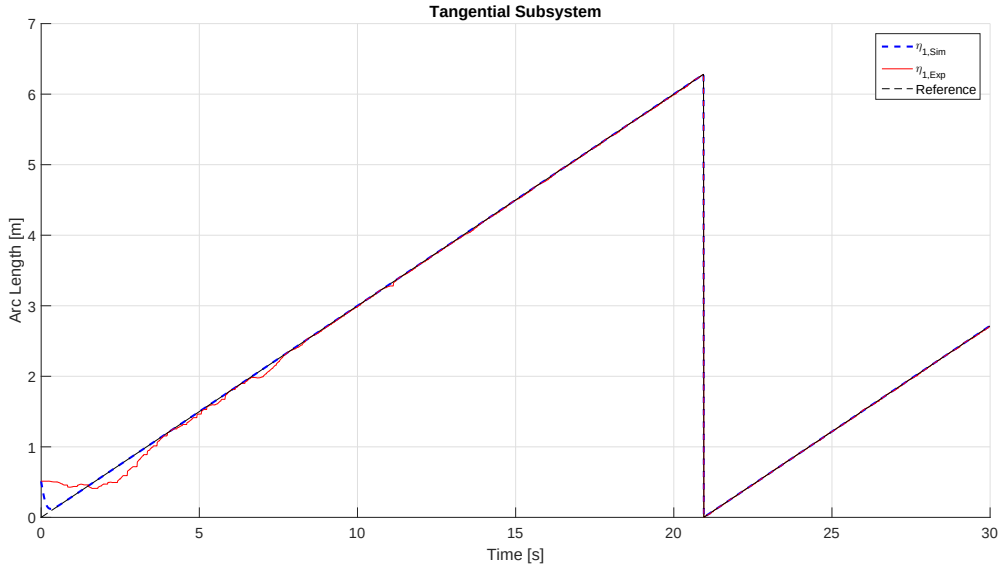

Figure 6.6: Tangential Subsystem (η) - Test Case 1

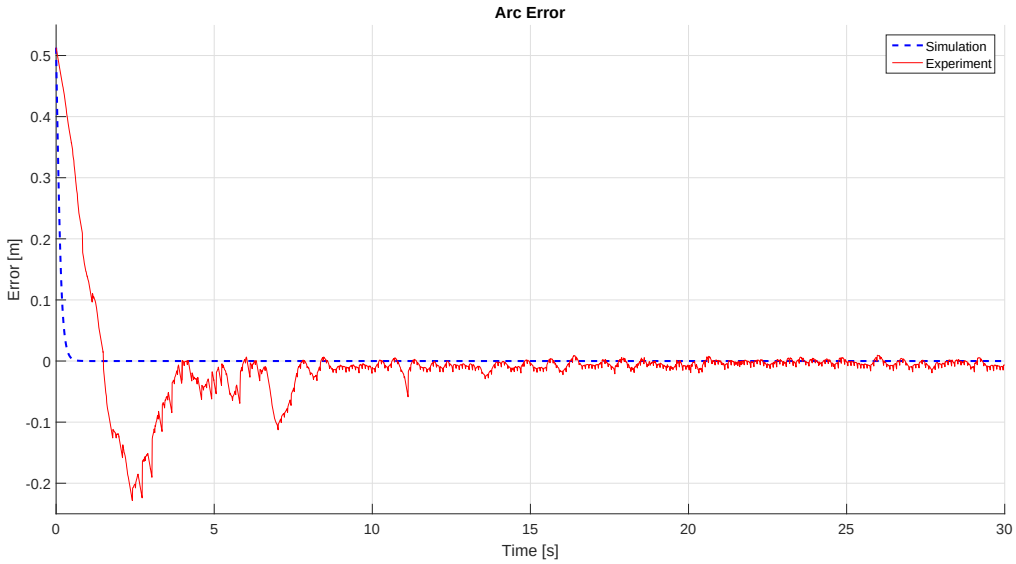

Figure 6.7: Arc Error - Test Case 1

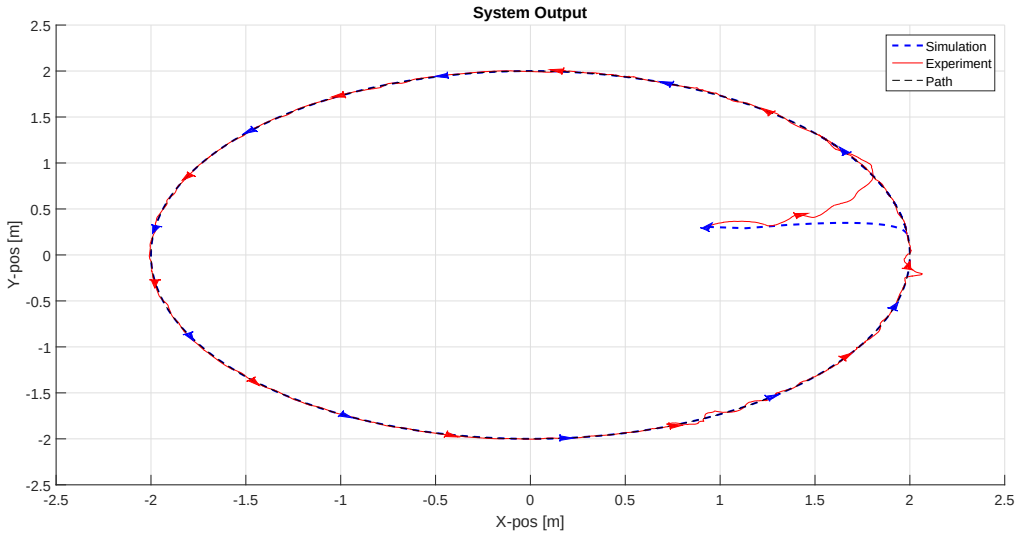

Figure 6.8: System Output - Test Case 2

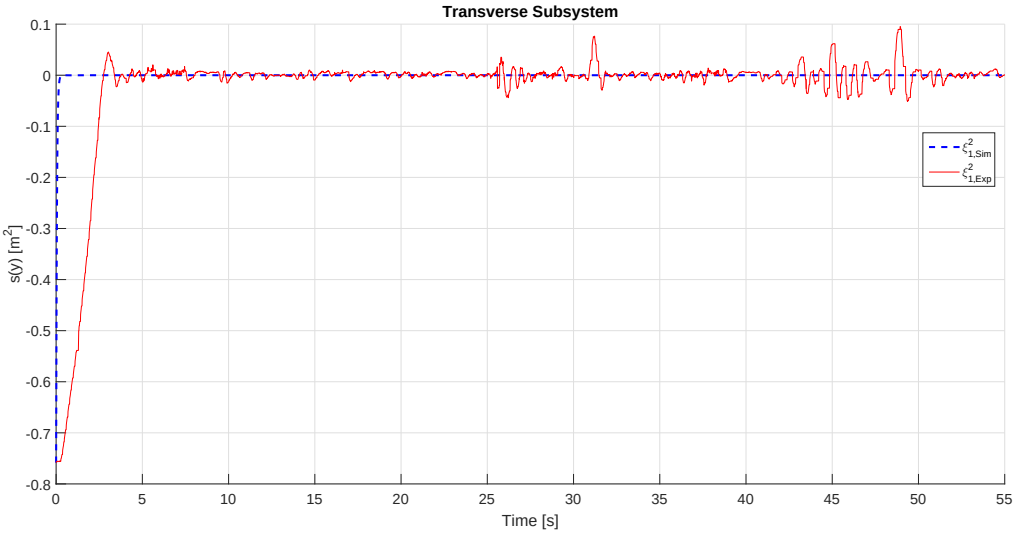

Figure 6.9: Transverse Subsystem (ξ) - Test Case 2

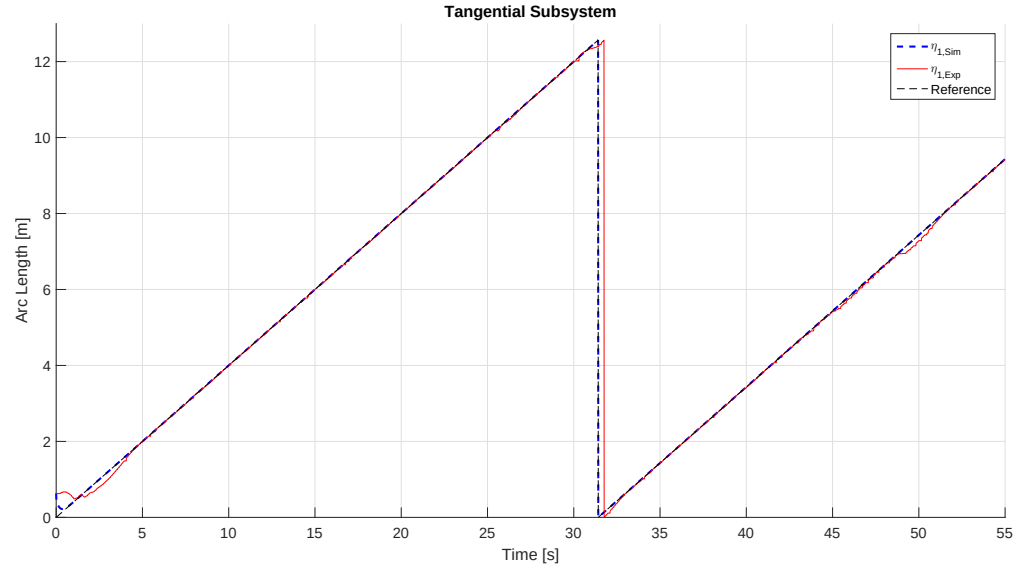

Figure 6.10: Tangential Subsystem (η) - Test Case 2

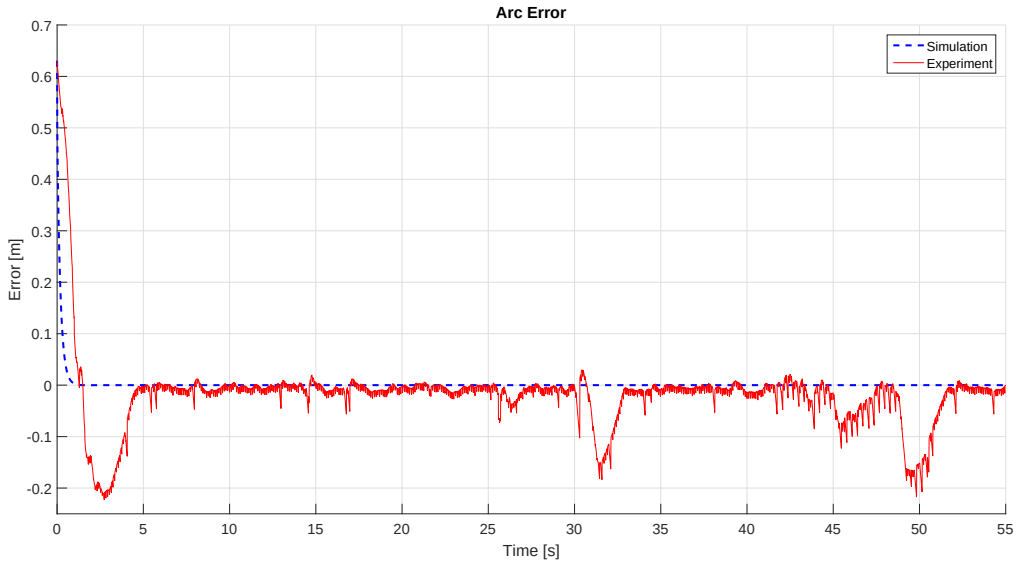

Figure 6.11: Arc Error - Test Case 2

Performance is inevitably worse in practice compared to simulation due to model uncertainty as discussed in Section 6.2 and noisy sensor measurements. The VICON camera system uses I.R. markers placed on the robot to sense positional information. A misalignment of I.R. markers can be devastating for performance because the feedback control depends on the position and orientation of the robot.

6.4.1 Alternative Implementation

As one of our motivating applications deals with autonomous vehicles, we consider an augmented control algorithm to accommodate some practical considerations. Laboratory results could not be collected so only simulation results will be shown. The path following objective is primarily interested in driving the system output to an assigned curve. Secondarily, a reference for the curve should be followed. For this reason, we slightly modify

the controller logic and first stabilize the system output to the point closest on the curve. This is easily accomplished by stabilizing

$$\eta_2 = \cdots = \eta_r = v^{\|} = 0$$

so that the closest point on the path doesn't change very much over time.

A typical motion for an agent is to loop around its designated path continuously. Once the system output is near the path ($\|\xi\| < \epsilon_1$, $\epsilon_1 > 0$), the system should wait for $\|e_{\text{arc}}\| \to 0$. After $\|e_{\text{arc}}\| < \epsilon_2$, $\epsilon_2 > 0$ the controller discussed in Chapter 4 can be implemented.

Instead of continuing towards the path exponentially with $v^{\|} = 0$, once the reference is close enough the tangential subsystem controller is switched to

$$v^{\|} = K_\eta \mathbf{e} + \frac{\mathrm{d}^r}{\mathrm{d}t^r} Q w(\theta).$$

This is advantageous because now the system output is quickly forced to a point on its path and remains there until the reference is near. This helps lower the overall control effort used and diminishes the distance traveled off of the curve.

Simulated results illustrating this idea are shown in the figures below. Stability of the transversal subsystem can be seen in Figure 6.13. The new behavior exhibited in regards to tracking is shown in Figure 6.14. Parameter values are the same as those in Table 6.2.

Test Case	R [m]	$x_1(0)$ [m]	$x_2(0)$ [m]	$x_3(0)$ [rad]	$w_1(0)$	$w_2(0)$
3	1	1.96	-0.97	3.04	0	0.2

Table 6.3: Alternate Single Agent Initial Conditions

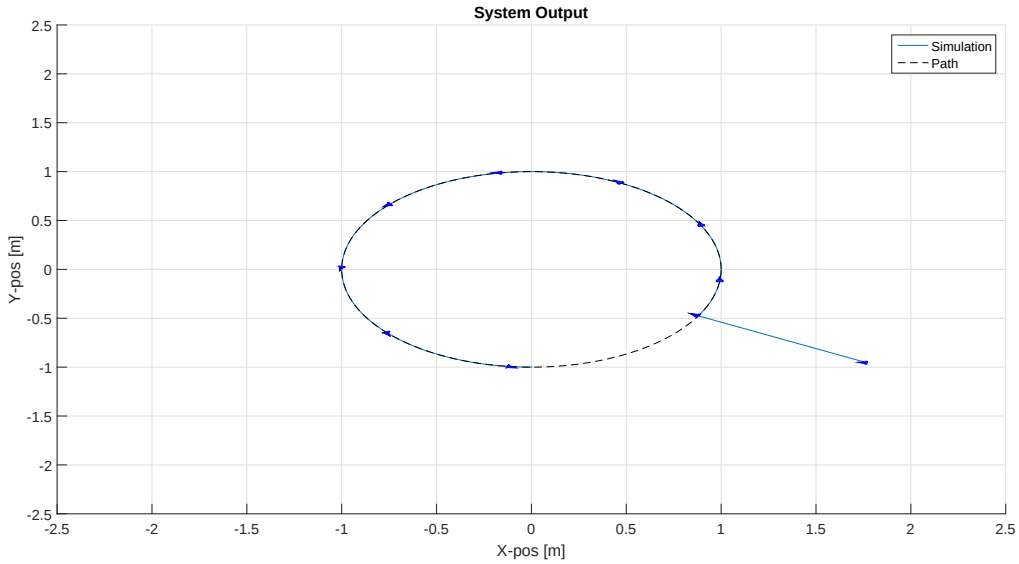

Figure 6.12: System Output - Test Case 3

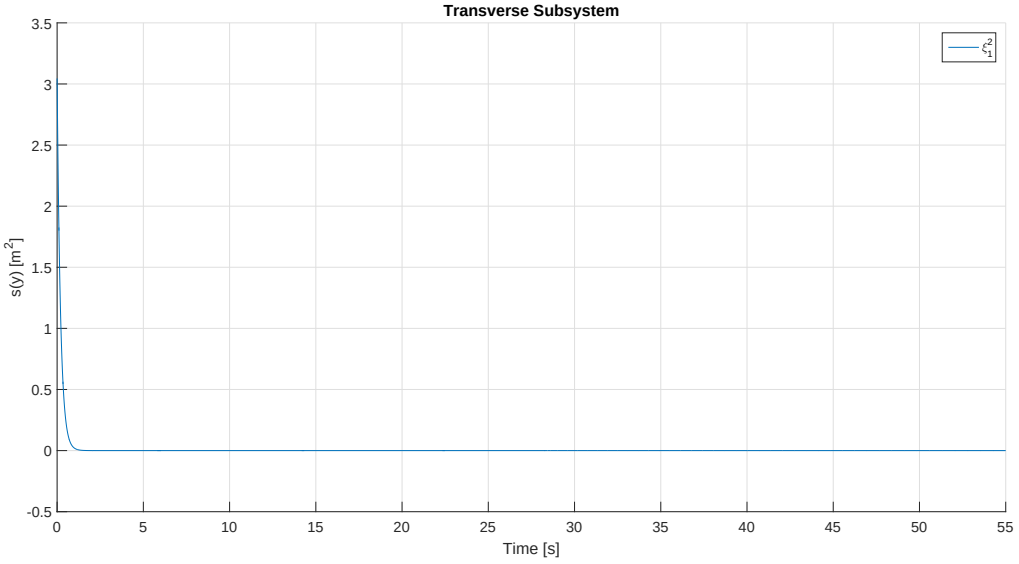

Figure 6.13: Transverse Subsystem (ξ) - Test Case 3

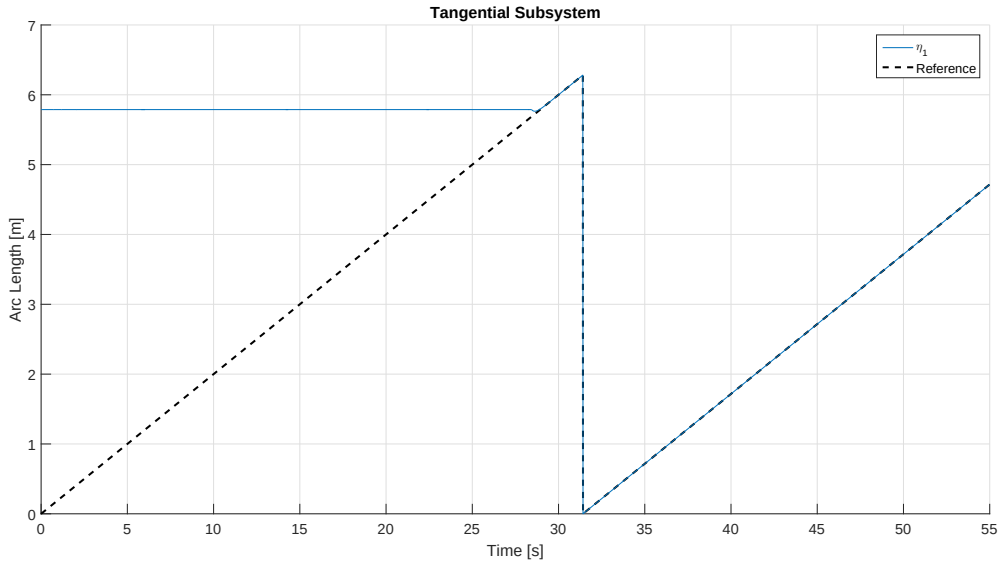

Figure 6.14: Tangential Subsystem (η) - Test Case 3

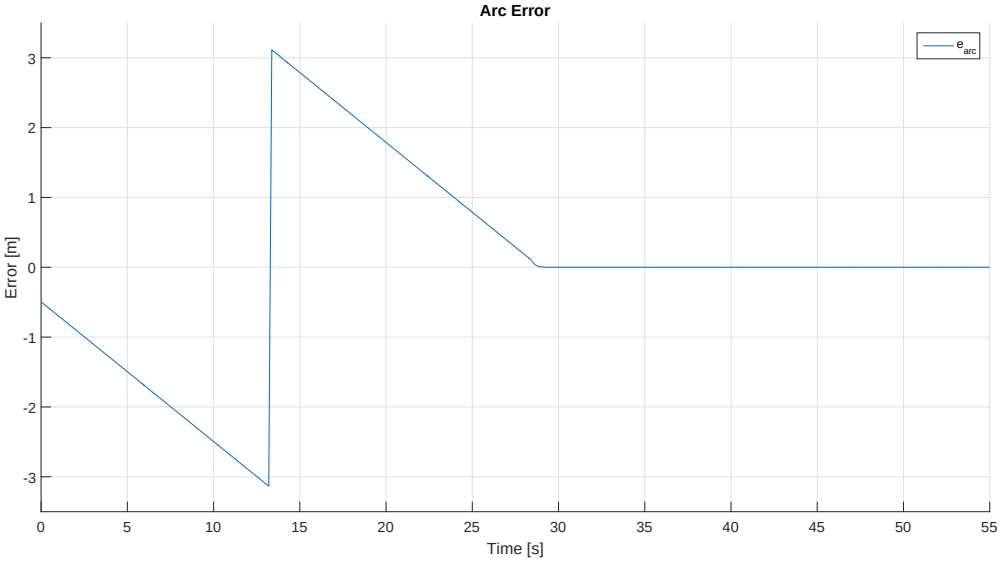

Figure 6.15: Arc Error - Test Case 3

6.5 Synchronized Path Following

We now illustrate the results of Chapter 5 in the laboratory. Each robot executes control law (5.7) from Theorem 5.2.5 while modifying their internal model of the exosystem according to the results of Theorem 5.2.3. We use the same θ, S and Q as in the previous section so that robot 1 has as its exosystem

$$\dot{w}_1 = \begin{bmatrix} 0 & 1 \\ 0 & 0 \end{bmatrix} w_1 + (w_2 - w_1)$$
$$r_1(t) = R_1 \begin{bmatrix} \cos\left(\mathrm{mod}(w_{1,1}(t), 2\pi)\right) \\ \sin\left(\mathrm{mod}(w_{1,1}(t), 2\pi)\right) \end{bmatrix}.$$

and robot 2 uses

$$\dot{w}_2 = \begin{bmatrix} 0 & 1 \\ 0 & 0 \end{bmatrix} w_2 + (w_1 - w_2)$$
$$r_2(t) = R_2 \begin{bmatrix} \cos\left(\mathrm{mod}(w_{2,1}(t), 2\pi)\right) \\ \sin\left(\mathrm{mod}(w_{2,1}(t), 2\pi)\right) \end{bmatrix}.$$

Two test cases are shown. The differences between cases are highlighted in Table 6.4 with parameter values listed in Table 6.5. Stability of the ξ-subsystems and the synchronization in the η-subsystems is shown in the figures below.

Test Case	Agent	R_i [m]	$x_{i,1}(0)$ [m]	$x_{i,2}(0)$ [m]	$x_{i,3}(0)$ [rad]	$w_{i,1}(0)$	$w_{i,2}(0)$
4	1	2	-2.75	0.32	5.84	0	0.1
	2	1	-1.97	-1.43	0.37	0	0.3
5	1	2	1.31	-1.77	1.04	0	0.1
	2	1	-2.39	0.31	5.70	0	0.3

Table 6.4: Multi Agent Initial Conditions

Parameter	Value
K_ξ	-20
K_η	-10
$\theta(t)$	t
ℓ	0.2 [m]

Table 6.5: Multi Agent Parameter Values

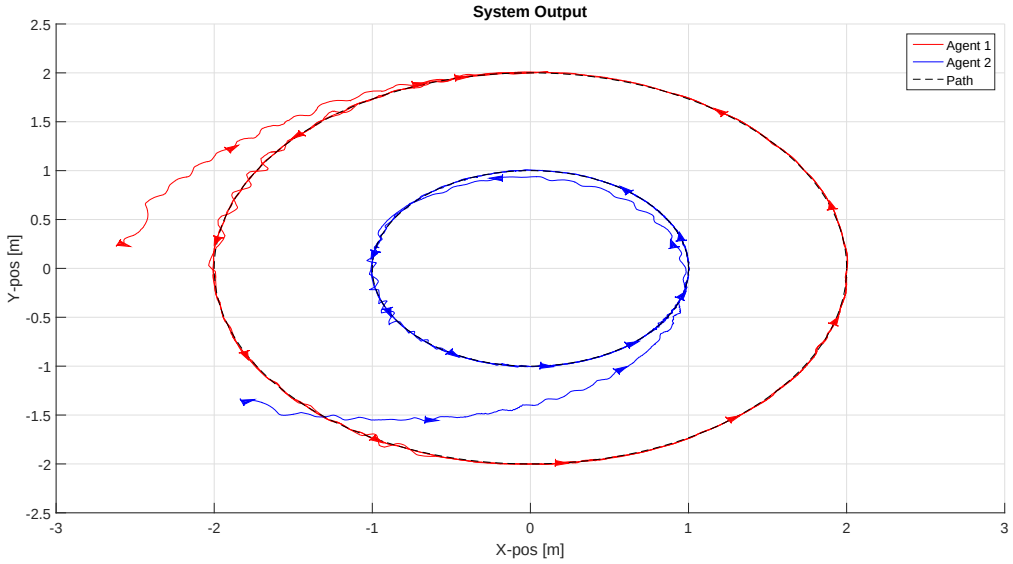

Figure 6.16: System Output - Test Case 4

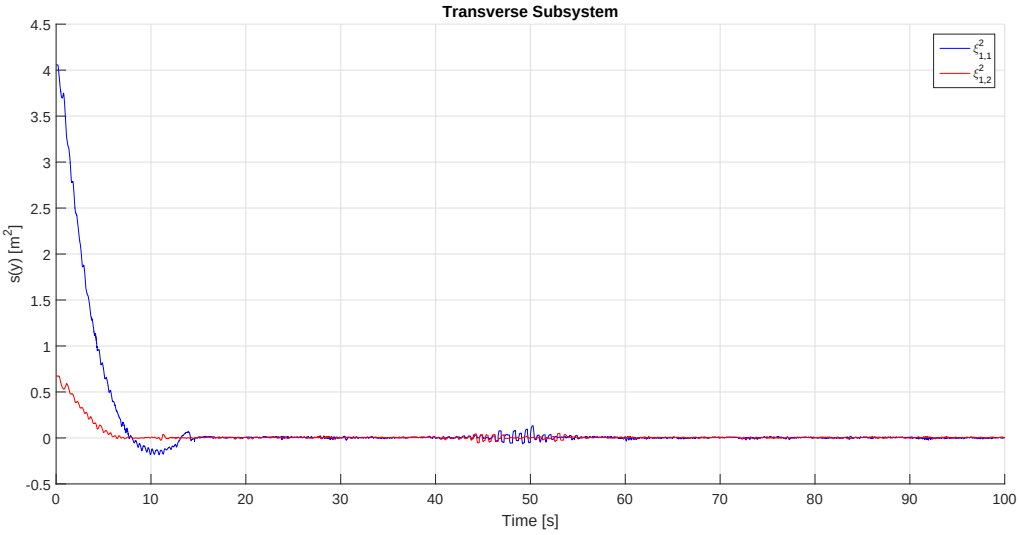

Figure 6.17: Transverse Subsystem (ξ) - Test Case 4

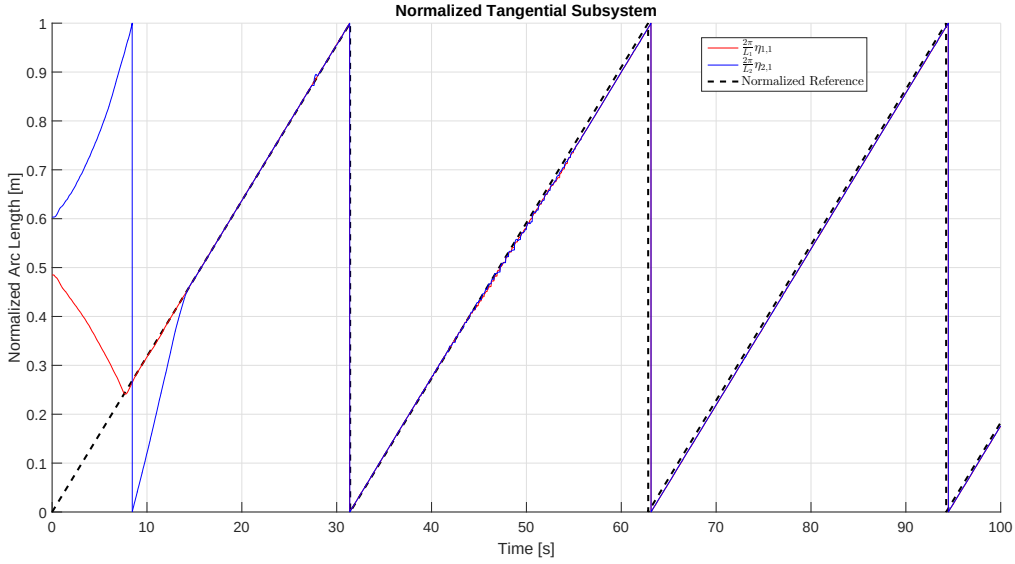

Figure 6.18: Normalized Tangential Subsystem (η) - Test Case 4

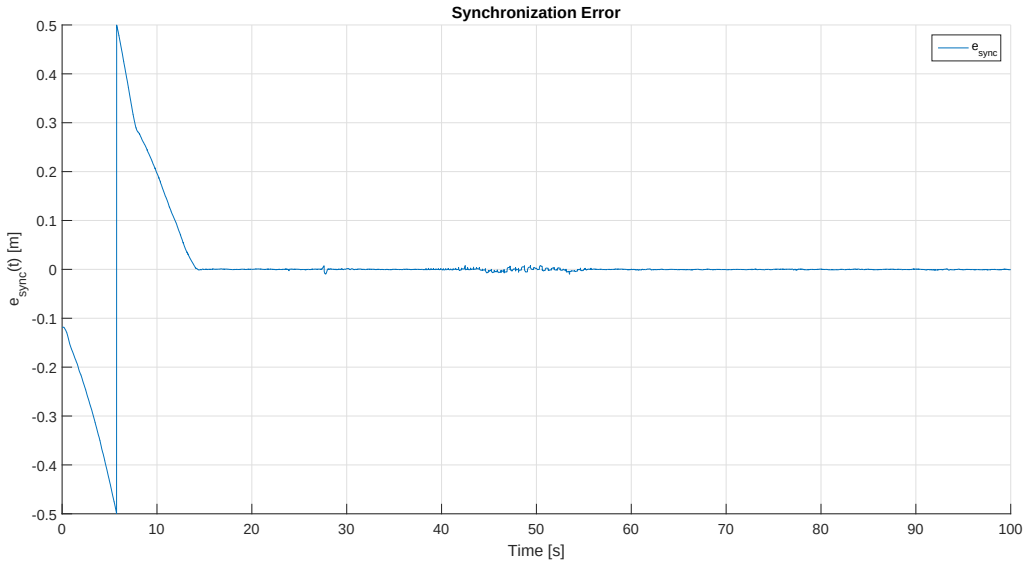

Figure 6.19: Synchronization Error - Test Case 4

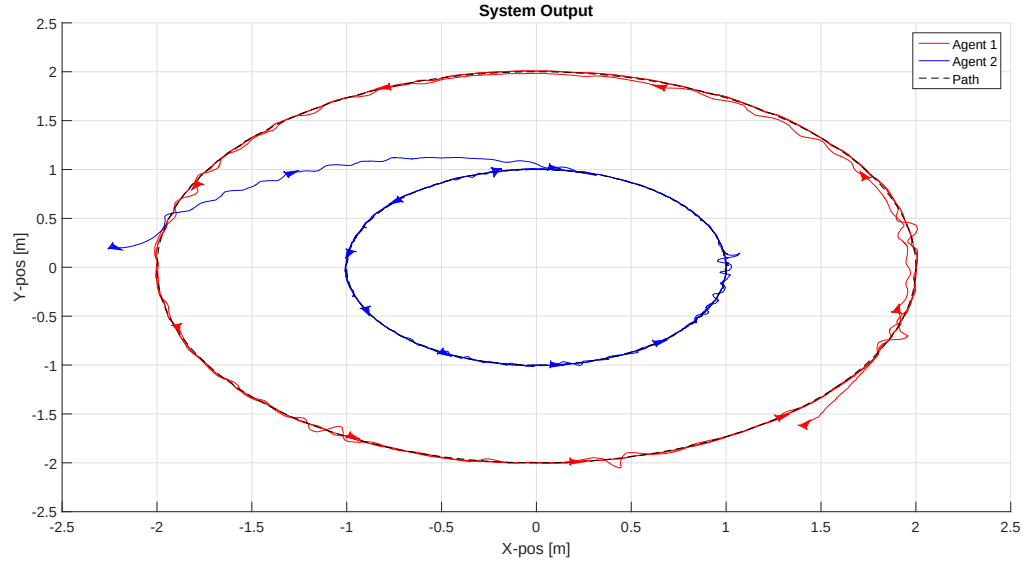

Figure 6.20: System Output - Test Case 5

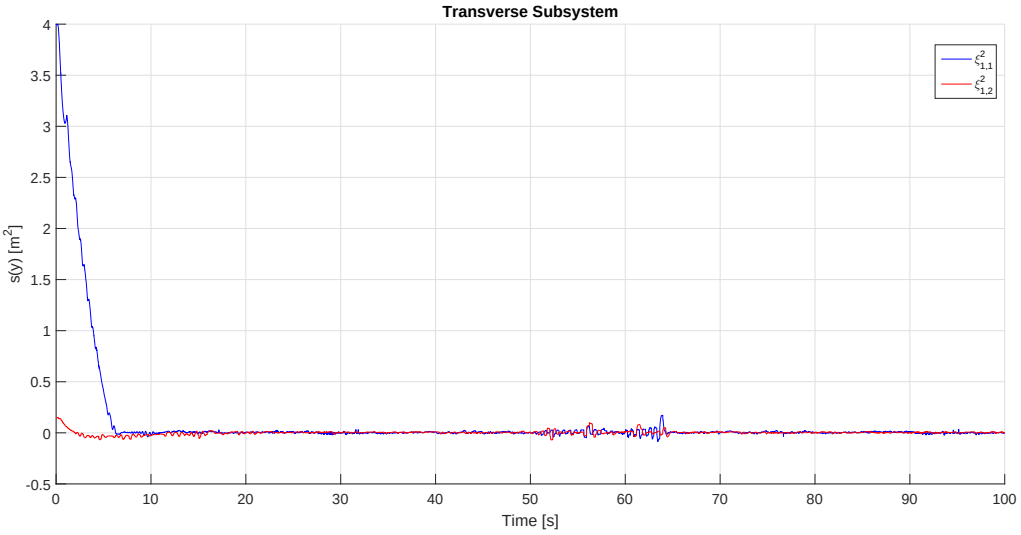

Figure 6.21: Transverse Subsystem (ξ) - Test Case 5

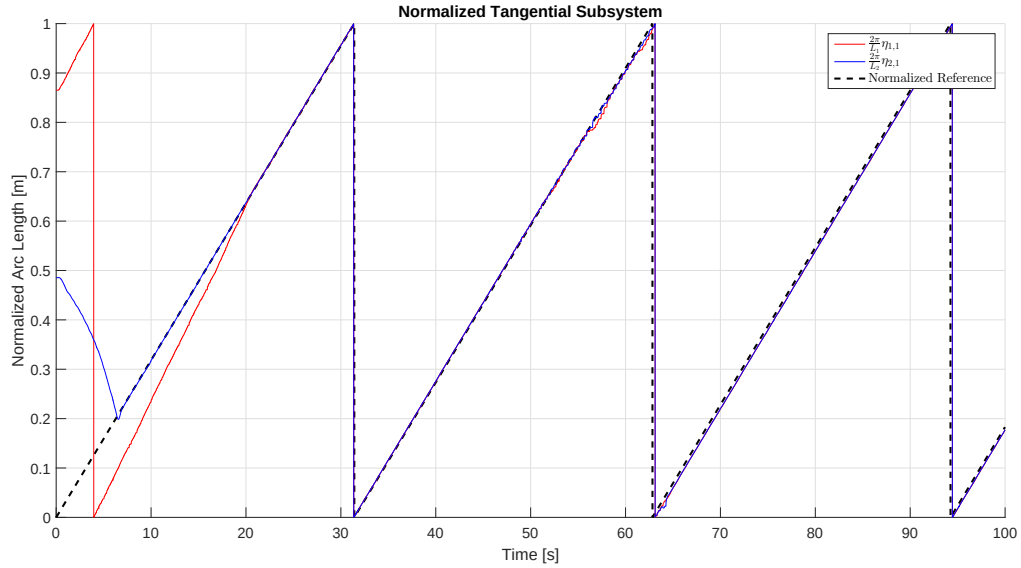

Figure 6.22: Normalized Tangential Subsystem ($\bar{\eta}$) - Test Case 5

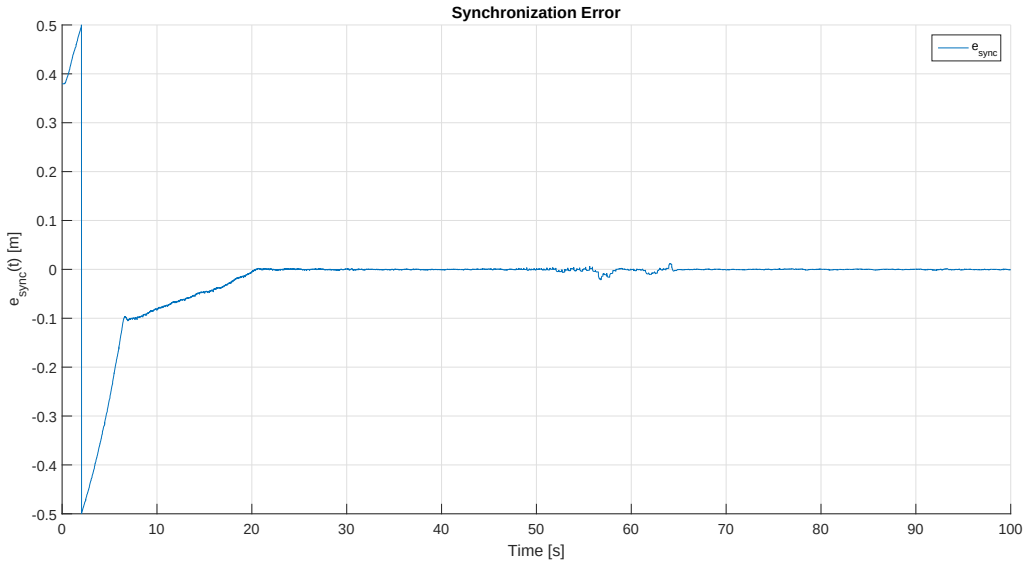

Figure 6.23: Synchronization Error - Test Case 5

Once more, performance is inevitably worse in practice compared to simulation. In addition to all the previous hindrances, the M.A.S. introduces communication delays and the possibility to collide with one another. Collisions are avoided at all costs by using appropriate initial conditions and ensuring each agent's output path is distinct with a sufficient separation between the paths at all times.

6.5.1 Alternative Considerations

Once again, a different situation is considered using autonomous vehicles as a basis for showcasing the practical potential possible using the control architecture. Laboratory results could not be collected so only simulation results will be shown. The path following objective is primarily interested in driving the system output to an assigned curve. In this case, the assigned curve of each system is identical. The secondary objective of the path

following problem is then to maintain a constant distance between each system. This is useful for allowing multiple cars to use the same lane of traffic.

Simulated results illustrating this idea are shown in the figures below. Stability of the transversal subsystem can be seen in Figure 6.25. The new behavior exhibited in regards to tracking is shown in Figure 6.27. Parameter values are the same as those in Table 6.5.

Test Case	Agent	R_i [m]	$x_{i,1}(0)$ [m]	$x_{i,2}(0)$ [m]	$x_{i,3}(0)$ [rad]	$w_{i,1}(0)$	$w_{i,2}(0)$
6	1	2	0.7	-1.5	5	0	0.2
	2	2	2.1	1.7	2	0	0.4

Table 6.6: Multi Agent Initial Conditions

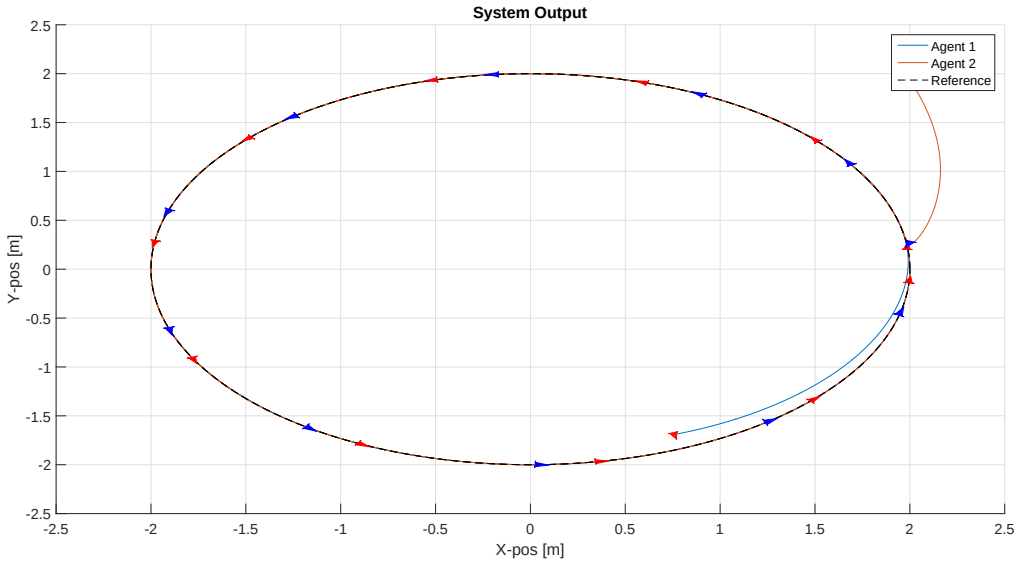

Figure 6.24: System Output - Test Case 6

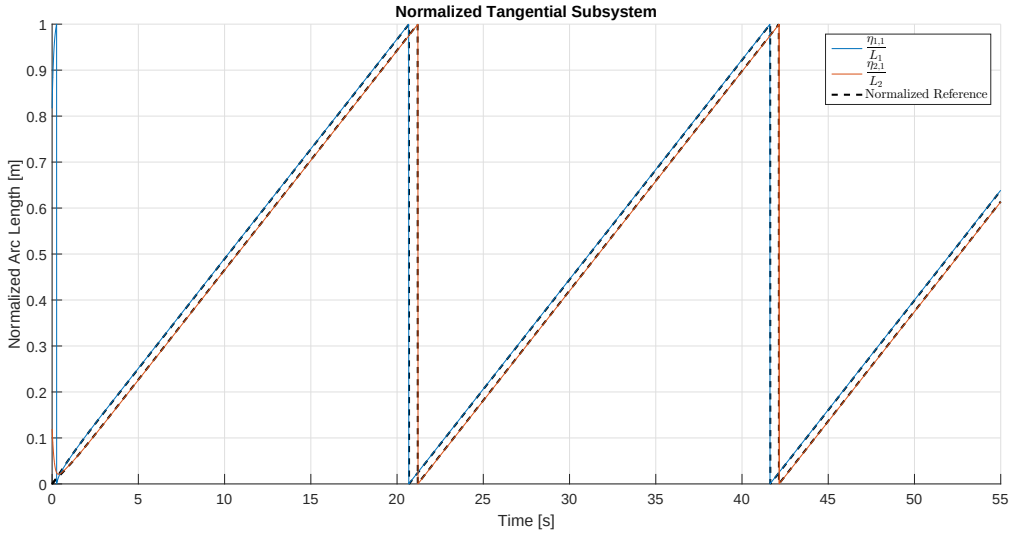

Figure 6.25: Transverse Subsystem (ξ) - Test Case 6

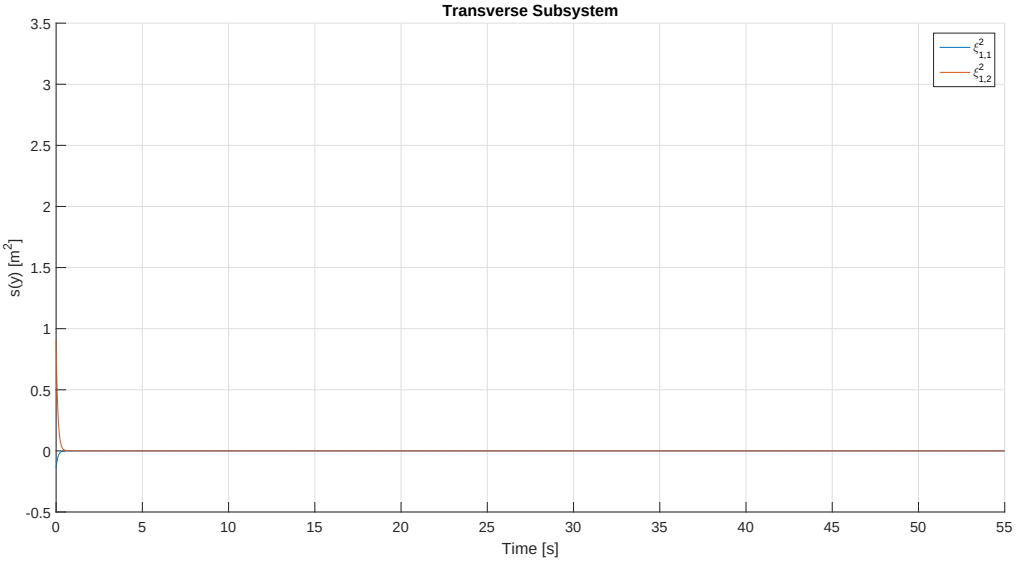

Figure 6.26: Tangential Subsystem (η) - Test Case 6

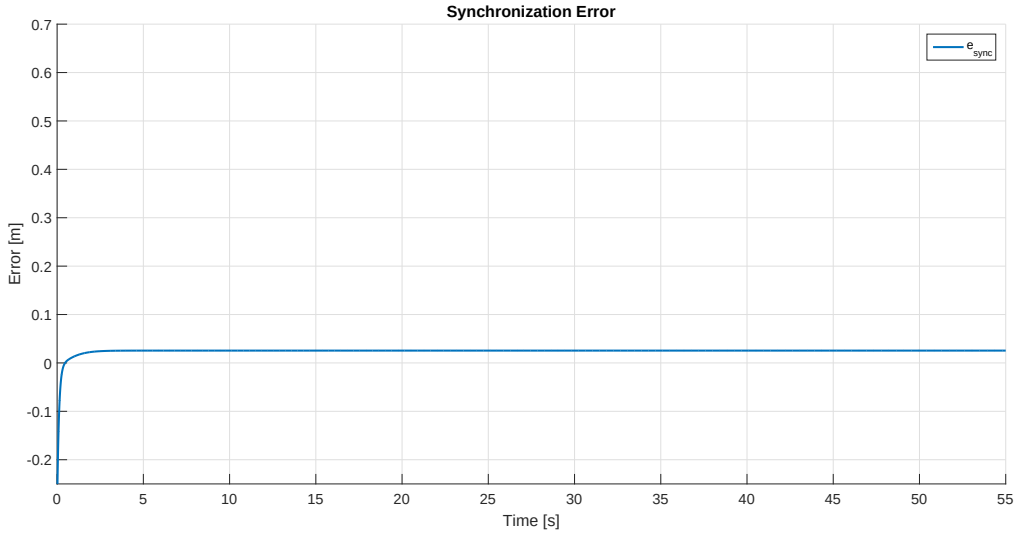

Figure 6.27: Synchronization Error - Test Case 6

The simulation does not take into account collisions and simply allows the vehicles to pass through one another. Although this is not practical, more advanced algorithms could always be implemented to accommodate collision avoidance without degrading the integrity of the control algorithm itself.

Consistent with Definition 5.2.1, the steady state error in Figure 6.27 shows that the two systems maintain a constant distance apart while traversing the curve. This distance is also measured in revolutions of the path.

Chapter 7

Conclusions and Future Research

7.1 Conclusions

In this thesis, we applied output synchronization techniques to the path following control design problem. A special normal form with useful characteristics aids our process. Furthermore, some mild attention is placed on performance limitations for individual N.M.P. systems in the context of path following. Chapter 3 provides the path following outputs and normal form, essential tools used in the development of a solution. The path following outputs define the system's original output in transformed coordinates for a useful physical meaning. They represent the minimum distance to the path and how far the system has traversed the path relative to an initial starting point. The normal form is then used as the basis for controller design. In Chapter 4 only a single system is considered with the objective of getting to the path and enforcing invariance of the path. In the case of N.M.P. systems, the purposed control law is augmented to allow for increased performance by way of [1]. Chapter 5 extends the single agent case to a M.A.S.. By altering each system's

reference, a common normalized trajectory is found that all agents must follow. Following [41], a consensus algorithm is used on the references to make them identical. The internal model principal is observed to be satisfied and synchronization is achieved. Simulation and experimental results are presented in Chapter 6. The physical experiment acts to further simulation results by introducing a real world environment with time delays in communication, friction and many other unmodeled dynamics. In practice the purposed control law is seen to work within a reasonable degree of error.

7.2 Future Research

It would be interesting to apply the results of [1] to the M.A.S. case in which the agents were N.M.P.. Since the control algorithms for path following and synchronization are decoupled there are a number of ways both [1] and [41] could be applied. It could be that both algorithms are run simultaneously from the very beginning. Another implementation could be to run the step-down approach of [1] for an agreed upon length of time. Then afterwards, agents are guaranteed to be on their respective paths with decreased arc error. Afterwards, the agents use the communication graph to exchange information regarding their references in order to synchronize.

Minimizing synchronization and arc error simultaneously could then be investigated. All the underlying theory presented can be executed by individual systems sharing a common normalized path following output. It is unnecessary that each system be identical and different types of autonomous vehicles could be used producing a heterogenoeous M.A.S.. Assumption 4 imposes strict characteristics of the interconnection graph used by the M.A.S.. As the number of agents in the M.A.S. increases, less stringent, time varying interconnection graphs could be explored.

Secondly, mostly all of the results presented in Chapter 6 use only two agents with non-intersecting circular paths. Application in which collision avoidance and safety are number one priorities could benefit from more intricate output paths with possible intersection. The distributed nature of the solution could also be showcased by using a larger M.A.S..

Lastly, applying the algorithms discussed in this thesis on real world highways could be explored. Although Assumption 1 imposes strong geometric constraints on the type of paths considered theoretically; practically all that is needed is for the curve to be as differentiable as the transverse subsystem. This means that splines could be used to piece together a real world highway. Once complete, all the geometric properties associated with each spline segment would be used to implement the final controller.

References

[1] A. P. Aguiar, J. P. Hespanha, and P. V. Kokotović. Path-following for non-minimum phase systems removes performance limitations. *IEEE Transactions on Automatic Control*, 50(2):234–239, 2005. 2, 4, 95, 96

[2] A. P. Aguiar, J. P. Hespanha, and P. V. Kokotović. Performance limitations in reference tracking and path following for nonlinear systems. *Automatica*, 44(3):598–610, 2008. 5, 47

[3] A. P. Aguiar and J.P. Hespanha. Trajectory-tracking and path-following of underactuated autonomous vehicles with parametric modeling uncertainty. *IEEE Transactions on Automatic Control*, 52(8):1362–1379, 2007.

[4] A. Akhtar, C. Nielsen, and S. Waslander. Path following using dynamic transverse feedback linearization for car-like robots. *IEEE Transactions on Robotics*, 31(2), 2015.

[5] G. Bastin, B. Siciliano, and C. C. de Wit. *Theory of Robot Control*. Springer, 1996.

[6] F. Blanchini. Set invariance in control. *Automatica*, (35):1747–1767, 1999.

[7] L. Consolini, M. Maggiore, C. Nielsen, and M. Tosques. Path following for the pvtol aircraft. *Automatica*, 46(8):1284–1296, 2010. 29

[8] E.J. Davison and S.H. Wang. Properties and calculation of transmission zeros of linear multivariable systems. *Automatica*, 10:643–658, 1974. 26

[9] A. Doosthoseini and C. Nielsen. Local nested transverse feedback linearization. *Mathematics of Control, Signals, and Systems*, 27:493–522, 2015. 2, 28

[10] Alireza Doosthoseini and Christopher Nielsen. Coordinated path following for a multi-agent system of unicycles. In 52^{nd} *IEEE Conference on Decision and Control*, pages 2894–2899, 2013. 7

[11] B. Francis. The linear multivariable regulator problem. *SIAM J. Control and Optimization*, 15(3):486–505, 1977.

[12] B.A. Francis and W.M. Wonham. The internal model principle of control theory. *Automatica*, 12:457–465, 1976. 7

[13] V. Guillemin and A. Pollack. *Differential Topology*. Prentice Hall, New Jersey, 1974. 34, 41

[14] A. Hladio, C. Nielsen, and D. Wang. Path following for a class of mechanical systems. *IEEE Transactions on Control Systems Technology*, 21:2380–2390, 2013. 32

[15] R. A. Horn and C. R. Johnson. *Topics in Matrix Analysis*. Cambridge University Press, 1991.

[16] J. Huang and Ching-Fang Lin, editors. *Internal Model Principle and Robust Control of Nonlinear Systems*, 9131 Mason Ave., Chatsworth, CA 91311, 1993. American GNC Corporation. Proceedings of the 32^{nd} Conference on Decision and Control.

[17] A. Isidori. *Nonlinear Control Systems*. Springer, Secaucus, NJ, USA, 1995. 16, 17, 24, 35, 36

[18] A. Isidori. *Nonlinear Control Systems II*. Springer, London, 1999. 24, 40

[19] A. Isidori. *Lectures in Feedback Design for Multivariable Systems*. Springer, 2017. 24, 64

[20] A. Jadbabaie, J. Lin, and A. S. Morse. Coordination of groups of mobile autonomous agents using nearest neighbour rules. *IEEE Transactions on Automatic Control*, 48:988–1001, 2003.

[21] S. H. Juan and F. H. Cotarelo. Multi-master ros systems. 2015. 74

[22] H. Kwakernaak and R. Sivan. The maximally achievable accuracy of linear optimal regulators and linear optimal filters. *IEEE Transactions on Automatic Control*, 17(1):79 – 86, 1972. 4

[23] Harry Kwatny. *Nonlinear control and analytical mechanics : a computational approach*. Birkhauser, Boston, 2000. 19

[24] J.M. Lee. *Introduction to Smooth Manifolds*. Springer-Verlag, 2002. 33, 105, 106

[25] Y. Li and C. Nielsen. Synchronized closed path following for a differential drive and manipulator robot. *IEEE Transactions on Control Systems Technology*, 25(2):704–711, 2016. 2, 28

[26] D. E. Miller and R.H. Middleton. c. *IEEE Transactions on Automatic Control*, 52(11):2586–2601, 2008. 2, 6, 24, 52

[27] L. Moreau, editor. *Stability of Continuous-Time Distributed Consensus Algorithms*, Ghent, Belgium, December 14-17 2004. Sidmar. Atlantis, Paradise Island, Bahamas.

[28] L. Moreau. Stability of multiagent systems with time-dependent communication links. *IEEE Transactions on Automatic Control*, 50(2):169–182, 2005.

[29] J. Munkres. *Topology*. Pretice-Hall, Toronto, ON, Canada, 2^{nd} edition, 2000. 105

[30] C. Nielsen, C. Fulford, and M. Maggiore. Path following using transverse feedback linearization: Application to a maglev positioning system. *Automatica*, 46(3):585–590, 2010.

[31] C. Nielsen and M. Maggiore. On local transverse feedback linearization. *SIAM Journal on Control and Optimization*, 47(5):2227–2250, 2008.

[32] H. Nijmeijer and A. van der Schaft. *Nonliner Dynamical Control Systems*. Springer - Verlag, New York, U.S.A., 1990. 10

[33] R. Olfati-Saber and R. Murray. Consensus problems in networks of agents with switching topology and time-delays. *IEEE Transactions on Automatic Control*, 49(9):1520–1533, 2004.

[34] C. Persis and B. Jayawardhana. On the internal model principle in the coordination of nonlinear systems. *IEEE Transactions on Control of Netowrk Systems*, 1(3):272–282, 2014.

[35] E. Protalinski. Googles self-driving cars have autonomously driven over 1 million miles. *venturebeat*, 2015. 2

[36] L. Qiu and J. Davison. Performance limitations of non-minimum phase systems in the servomechanism problem. *Automatica*, 29(2):337 – 349, 1993. 4, 5

[37] L. Scardovi and R. Sepulchre. Synchronization in networks of identical linear systems. *Automatica*, 45(11):2557–2562, 2009. 2, 6, 63, 65

[38] M. M. Seron, J. H. Braslavsky, P. V. Kokotović, and D. Q. Mayne. Feedback limitations in nonlinear systems: From bode integrals to cheap control. *IEEE Transactions on Automatic Control*, 44(4):829–833, 1999.

[39] H. Shim, J. Lee, J.-S. Kim, and J. Back, editors. *Output Regulation Problem and Solution for LTV Minimum Phase Systems with Time-varying Exosystem*, Bexco, Busan, Korea, Oct 18-21 2006. SICE-ICASE International Joint Conference.

[40] R. Skjetne, T. Fossen, and P. V. Kokotović. Robust output maneuvering for a class of nonlinear systems. *Automatica*, 40:373–282, 2004.

[41] P. Wieland, R. Sepulchre, and F. Allgöwer. An internal model principle is necessary and sufficient for linear output synchronization. *Automatica*, 47:1068–1074, 2011. 2, 7, 61, 63, 96

APPENDICES

Appendix A

Miscellaneous Proofs

A.1 Proposition 3.2.5

Proof. Let $F^{-1} : N \to M$ denote the smooth inverse of F. Then $F \circ F^{-1} = I_N$ and $F^{-1} \circ F = I_M$. Differentiating these expressions and applying the chain rule for manifolds we have that, for each $p \in M$, $I = \mathrm{d}(F \circ F^{-1})_{F(p)} = \mathrm{d}F_p \circ \mathrm{d}F^{-1}_{F(p)}$ and $I = \mathrm{d}(F^{-1} \circ F)_p = \mathrm{d}F^{-1}_{F(p)} \circ \mathrm{d}F_p$. Thus $\mathrm{d}F_p$ is invertible and therefore it is an isomorphism between vector spaces. □

A.2 Proposition 3.2.8

Proof. The map $F : M \to F(M)$ is surjective since we've restricted its codomain. It is injective by hypothesis thus $F : M \to F(M) \subseteq N$ is bijective and therefore has an inverse $F^{-1} : F(M) \to M$. We are left to show that F and F^{-1} are smooth.

Let $p \in M$ be arbitrary. Since F is a local diffeomorphism there exists an open set $U \subseteq M$ containing p which F maps diffeomorphically onto $F(U) \subset N$. Without loss of generality, shrinking U if necessary, let (U, φ) be a coordinate neighbourhood of M about p and let $(F(U), \psi)$ be a coordinate neighbourhood of N about $F(p)$. Then, since F is a local diffeomorphism, we have that $\hat{F} = \psi \circ F \circ \varphi^{-1}$ and $\hat{F}^{-1} = \varphi \circ F^{-1}\psi^{-1}$ are smooth functions between Euclidean spaces. Applying Definition 3.2.3 and noting that $p \in M$ was arbitrary, we conclude that F and F^{-1} are smooth functions. □

A.3 Theorem 3.2.9

Proof. Since $\mathrm{d}F_p$ is an isomorphism at each $p \in S$, by Theorem 3.2.6 there exists an open set U_p containing p on which $F : U_p \to F(U_p)$ is a diffeomorphism. The collection of open sets $\{U_p\}_{p \in S}$ is an open cover of S. Since S is compact, there exists a finite subcover of S. Denote this subcover by $\{U_i\}_{i \in \mathbb{N}_N}$ for some finite natural number N and define $U := \cup_{i=1}^{N} U_i$. Again, by Theorem 3.2.6, F is a local diffeomorphism at each $p \in U$. Therefore, to prove the theorem we appeal to Proposition 3.2.8 and show that there exists an open set containing S on which F is one-to-one. If such a set exists, then by Proposition 3.2.8 F is a diffeomorphism onto its image with its domain taken to be the intersection U and this open set.

By way of contradiction, suppose that no such neighbourhood exists. First we construct a compact set containing S and contained in U. Every manifold is a locally compact Hausdorff space [24, Corollary 1.7]. Therefore, by [29, Theorem 29.2], given $p \in S \cap U_p$, where U_p is one of the sets from the (infinite) open cover constructed above, there exists a neighbourhood W_p of p such that the closure of W_p is compact and contained in U_p. Then $\{W_p\}_{p \in S}$ is an open cover of S with $W_p \subseteq U_p$. Since S is compact, there exists a finite

subcover. Denote this subcover by $\{W_i\}_{i\in\mathbb{N}_N}$ for some finite natural number N and define $W \coloneqq \cup_{i=1}^{N} W_i$. By construction $W \subseteq U$. Since the union of a finite number of compact sets is compact $\bar{W} \coloneqq \cup_{i=1}^{N} \mathrm{cl}\,(W_i)$, where $\mathrm{cl}\,(W_i)$ is the closure of W_i, is a compact set.

Let $\{V_i\}_{i\in\mathbb{N}}$ be a sequence of open sets with $S \subset V_i$, $V_i \subset \bar{W}$ and $V_{i+1} \subset V_i$ (strict inclusion). Let $\{a_i\}_{i\in\mathbb{N}}$ and $\{b_i\}_{i\in\mathbb{N}}$ be infinite sequences with a_i, $b_i \in V_i$. Since a_i, b_i belong to the compact set $\bar{W}$, each sequence $\{a_i\}_{i\in\mathbb{N}}$ and $\{b_i\}_{i\in\mathbb{N}}$ has a convergent subsequence with limit point, respectively, a, b. By construction of the sets V_i these limit points must belong to S. Since, by assumption, F is one-to-one on S, $a = b = p$. However this implies that F cannot be a local diffeomorphism at p which is a contradiction. □

A.4 Theorem 3.4.2

Proof. Since $\mathrm{d}F_p$ is an isomorphism at each $p \in S$, by Theorem 3.2.6 there exists an open set U_p containing p which F maps diffeomorphically onto $F(U_p) \subset N$.

The set $\{F(U_p)\}_{p\in S}$ forms an open cover of $F(S)$. Since every manifold is paracompact [24, Proposition 2.24], the open cover $\{F(U_p)\}_{p\in S}$ admits a locally finite refinement[1]. Let $\{V_i\}$ be a locally finite refinement of $\{F(U_p)\}_{p\in S}$. In each V_i, the function F has local inverse G_i, i.e., $G_i : V_i \to M$ is such that $F \circ G_i = I_{V_i}$.

Define $W \coloneqq \{q \in N : G_i(q) = G_j(q) \text{ whenever } q \in V_i \cap V_j\}$. On W, we can define a global inverse $G : W \to M$ of F via $G(q) = G_i(q)$ for any i such that $q \in V_i$. This is well-defined on W since $G_i(q) = G_j(q)$ whenever $q \in V_i \cap V_j$.

The set W contains $F(S)$ since F maps S diffeomorphically onto $F(S)$. Therefore

[1] Given an open cover $\{U_i\}$ of a manifold M, another open cover $\{V_i\}$ is called a **refinement** of $\{U_i\}$ if for each $V \in \{V_i\}$, there exists a $U \in \{U_i\}$ such that $V \subseteq U$. An open cover $\{U_i\}$ of M is **locally finite** if each point of M possesses a neighbourhood that intersects only a finite many of the sets V_i.

$G_i(q) = G_j(q) = F^{-1}(w)$ for any $q \in F(S)$. Now fix $p \in S$ and $F(p) \in F(S)$. We will show that W contains a neighbourhood V of $F(p)$. Since $\{V_i\}$ is a locally finite cover of $F(S)$, there exists a neighbourhood V of $F(p)$ which intersects only a finite number of the V_i. Re-indexing them if necessary, call them $V_1, \ldots, V_k$.

Then $\tilde{V} = V \cap V_1 \cap \cdots \cap V_k$ is the finite intersection of open sets containing $F(p)$ and therefore $\tilde{V}$ is open and contains $F(p)$. Moreover, on $\tilde{V}$, each of the functions G_i is an inverse: $G_i(\tilde{V}) \subset U_p$ for $i \in \{1, \ldots, k\}$. Since all the G_i agree on $\tilde{V}$ we have that $\tilde{V} \subset W$. □

A.5 Time derivative of the arc error

We prove that $\dot{e}_{\text{arc}}(t) = \dot{e}_1(t)$.

Proof. Direct calculations will be used to show the result. We have that

$$e_{\text{arc}} = \frac{L}{2\pi} \arg\left(\exp\left(j\frac{2\pi}{L}e_1\right)\right).$$

Taking the derivative of this expression using the chain rule gives

$$\begin{aligned}
\dot{e}_{\text{arc}} &= \frac{\mathrm{d}e_{\text{arc}}}{\mathrm{d}e_1}\frac{\mathrm{d}e_1}{\mathrm{d}t} \\
&= \frac{\mathrm{d}}{\mathrm{d}e_1}\left[\frac{L}{2\pi}\arg\left(\exp\left(j\frac{2\pi}{L}e_1\right)\right)\right]\frac{\mathrm{d}e_1}{\mathrm{d}t} \\
&= \frac{\mathrm{d}}{\mathrm{d}e_1}\left[\frac{L}{2\pi}\arg\left(\cos\left(\frac{2\pi}{L}e_1\right)+j\sin\left(\frac{2\pi}{L}e_1\right)\right)\right]\frac{\mathrm{d}e_1}{\mathrm{d}t} \\
&= \frac{\mathrm{d}}{\mathrm{d}e_1}\left[\frac{L}{2\pi}\tan^{-1}\left(\frac{\sin\left(\frac{2\pi}{L}e_1\right)}{\cos\left(\frac{2\pi}{L}e_1\right)}\right)\right]\frac{\mathrm{d}e_1}{\mathrm{d}t} \\
&= \frac{\mathrm{d}}{\mathrm{d}e_1}\left[\frac{L}{2\pi}\tan^{-1}\left(\tan\left(\frac{2\pi}{L}e_1\right)\right)\right]\frac{\mathrm{d}e_1}{\mathrm{d}t} \\
&= \frac{\mathrm{d}}{\mathrm{d}e_1}\left[\frac{L}{2\pi}\left(\frac{2\pi}{L}e_1\right)\right]\frac{\mathrm{d}e_1}{\mathrm{d}t} \\
&= \frac{\mathrm{d}e_1}{\mathrm{d}e_1}\frac{\mathrm{d}e_1}{\mathrm{d}t} \\
&= \frac{\mathrm{d}e_1}{\mathrm{d}t} \\
&= \dot{e}_1
\end{aligned}$$

□